PARKINSON'S DISEASE

A patient-based model of RNA mis-splicing uncovers treatment targets in Parkinson's disease

Ibrahim Boussaad[1]*, Carolin D. Obermaier[1,2]*, Zoé Hanss[1], Dheeraj R. Bobbili[1], Silvia Bolognin[1], Enrico Glaab[1], Katarzyna Wołyńska[3], Nicole Weisschuh[4], Laura De Conti[5], Caroline May[6], Florian Giesert[7,8,9], Dajana Grossmann[1], Annika Lambert[1], Susanne Kirchen[1], Maria Biryukov[1], Lena F. Burbulla[10], Francois Massart[1], Jill Bohler[1], Gérald Cruciani[1], Benjamin Schmid[2], Annerose Kurz-Drexler[7], Patrick May[1], Stefano Duga[11,12], Christine Klein[13], Jens C. Schwamborn[1], Katrin Marcus[6], Dirk Woitalla[14], Daniela M. Vogt Weisenhorn[7,9], Wolfgang Wurst[7,8,9,15], Marco Baralle[5], Dimitri Krainc[10], Thomas Gasser[2,16], Bernd Wissinger[4], Rejko Krüger[1,2,17,18]†

Parkinson's disease (PD) is a heterogeneous neurodegenerative disorder with monogenic forms representing prototypes of the underlying molecular pathology and reproducing to variable degrees the sporadic forms of the disease. Using a patient-based in vitro model of *PARK7*-linked PD, we identified a U1-dependent splicing defect causing a drastic reduction in DJ-1 protein and, consequently, mitochondrial dysfunction. Targeting defective exon skipping with genetically engineered U1-snRNA recovered DJ-1 protein expression in neuronal precursor cells and differentiated neurons. After prioritization of candidate drugs, we identified and validated a combinatorial treatment with the small-molecule compounds rectifier of aberrant splicing (RECTAS) and phenylbutyric acid, which restored DJ-1 protein and mitochondrial dysfunction in patient-derived fibroblasts as well as dopaminergic neuronal cell loss in mutant midbrain organoids. Our analysis of a large number of exomes revealed that U1 splice-site mutations were enriched in sporadic PD patients. Therefore, our study suggests an alternative strategy to restore cellular abnormalities in in vitro models of PD and provides a proof of concept for neuroprotection based on precision medicine strategies in PD.

INTRODUCTION

Parkinson's disease (PD) is increasingly recognized as a heterogeneous disorder, as reflected by its substantial phenotypic, neuropathological, and genotypic variability (*1*). Therefore, previous models considering PD as a single disease entity, although successful for developing symptomatic therapies that compensate for the dopaminergic deficit responsible for the motor symptoms of PD, fall short in terms of developing neuroprotective treatment strategies (*2*). Focusing on pathomechanisms and understanding the underlying molecular pathology of neurodegeneration is essential, and genetic stratification of patients into subgroups provides an important entry point for precision medicine (*3*). During the past 20 years, a substantial number of genes related to PD have been identified, including mutations in genes responsible for rare monogenic forms of PD. These monogenic forms of PD have become a valuable resource for PD research, because patient-based cell models display disease-specific cellular phenotypes recapitulating the phenotypes found in postmortem brain tissue (*4*). According to this concept, the validation of clinicogenetic subtypes of PD may be achieved based on rare but strong molecular signatures and subsequently applied to the different pathophysiological tiers within each disease subtype (*5*).

Mutations disrupting splicing in monogenic PD have recently come into focus, and variants predicted in silico to cause aberrant splicing have been described for *PINK1*, *PARK2*, *PARK7*, and *GBA* (*6*–*9*). Mutations in the DJ-1 encoding gene *PARK7* are a rare cause of early-onset PD (*10*). In this study, we identified and validated an exonic splicing mutation in *PARK7*, c.192G>C. This mutation was previously described as a missense mutation altering the protein sequence of DJ-1 (p.E64D) (*11*). Using patient-derived cellular models, we discovered that the mutation disrupts the binding motif of the small nuclear RNA (snRNA) U1 leading to exon skipping. We applied a genetic approach and developed a pharmacological intervention that rescued aberrant splicing and cellular phenotypes.

Furthermore, we show for the common sporadic form of PD that yet unrecognized mutations in U1 splicing sites are overrepresented in exomes from patients compared to controls. Our findings are in line with large-scale characterization of disease-associated mutations that found splicing mutations largely underestimated and open the door for a mechanism-based personalized medicine strategy in PD (*12*).

[1]LCSB, Luxembourg Centre for Systems Biomedicine, University of Luxembourg, 4362 Esch-Sur-Alzette, Luxembourg. [2]Department of Neurodegenerative Diseases and Hertie-Institute for Clinical Brain Research, University of Tübingen, 72076 Tübingen, Germany. [3]Department of Medical Genetics, Poznan University of Medical Sciences, 60-806 Poznan, Poland. [4]Molecular Genetics Laboratory, Institute for Ophthalmic Research, University Clinics Tübingen, 72076 Tübingen, Germany. [5]ICGEB—International Centre for Genetic Engineering and Biotechnology, Padriciano 99, 34149 Trieste, Italy. [6]Medizinisches Proteom-Center, Ruhr-University Bochum, 44801 Bochum, Germany. [7]Helmholtz Zentrum München, Ingolstaedter Landstr. 1, 85764 Neuherberg, Germany. [8]German Center for Neurodegenerative Diseases (DZNE), Site Munich, Feodor-Lynen-Str. 17, 81377 Munich, Germany. [9]Technische Universität München-Weihenstephan, Developmental Genetics, c/o Helmholtz Zentrum München, Ingolstädter Landstr. 1, 85764 Neuherberg, Germany. [10]Department of Neurology, Northwestern University Feinberg School of Medicine, Chicago, IL 60611, USA. [11]Department of Biomedical Sciences, Humanitas University, Via Manzoni 113, 20089 Rozzano, Milan, Italy. [12]Humanitas Clinical and Research center, IRCCS, Via Manzoni 56, 20089 Rozzano, Milan, Italy. [13]Institute of Neurogenetics, University of Luebeck, 23562 Luebeck, Germany. [14]Department of Neurology, St. Josef-Hospital, Ruhr-University Bochum, 44791 Bochum, Germany. [15]Munich Cluster for Systems Neurology (SyNergy), Feodor-Lynen-Str. 17, 81377 Munich, Germany. [16]German Center for Neurodegenerative Diseases (DZNE), 72076 Tübingen, Germany. [17]Department of Neurology and Parkinson Research Clinic, Centre Hospitalier de Luxembourg (CHL), 1210 Luxembourg, Luxembourg. [18]Transversal Translational Medicine, Luxembourg Institute of Health (LIH), 1445 Strassen, Luxembourg.
*These authors contributed equally to this work.
†Corresponding author. Email: rejko.krueger@uni.lu

RESULTS

DJ-1 protein amount is reduced in carriers of the homozygous c.192G>C mutation

The c.192G>C mutation in *PARK7* was discovered in a family (*11*) and predicted to cause the amino acid change p.E64D. Subsequent studies conducted with E64D DJ-1 recombinant protein revealed only subtle effects on protein stability (*13*, *14*). Later, fibroblasts from family members became available, including from individual II.6 [who has severe depression (hom1)] and the index patient II.8 (hom2), both homozygous c.192G>C mutation carriers, as well as from an unaffected brother II.4 (het1) and the unaffected individual III.4 (het2), both heterozygous mutation carriers (Fig. 1A). Native fibroblasts of the homozygous mutation carriers (hom1 and hom2) showed a pronounced loss of DJ-1 protein to an almost undetectable quantity, whereas cells of heterozygous individuals intermediate DJ-1 quantities (Fig. 1B). Fibroblasts of both heterozygous individuals were still in the normal range of DJ-1 protein expression observed in a larger set of healthy donors (fig. S1A). To investigate the reduction in DJ-1 protein amounts across cell types, we reprogrammed fibroblasts to induced pluripotent stem cells (iPSCs) (fig. S2, A to D). iPSC clones (het1-3, hom1-4, hom2-1, and hom2-4) were further differentiated to small-molecule neural precursor cells (smNPCs) (*15*) that expressed the neuronal precursor markers SOX1 and NESTIN (fig. S2E). iPSC and smNPC were used to derive patient-specific neurons (*15*, *16*). DJ-1 protein amounts were markedly reduced in all iPSC (Fig. 1C), smNPC (Fig. 1D and fig. S1B), and iPSC-derived neurons (Fig. 1E) with the homozygous c.192G>C mutation. To test whether increased proteasomal or autophagy-lysosomal degradation pathways contribute to the reduction of the predicted E64D DJ-1 protein in homozygous mutation carriers, we blocked these pathways in smNPC. However, none of the inhibitors rescued DJ-1 protein in the homozygous mutation carriers (Fig. 1, F and G). To exclude the possibility that the lack of signal in the Western blot was due to the lower affinity of the antibody to the mutant protein, we tested two additional monoclonal antibodies binding different epitopes of DJ-1 and independently used mass spectrometry for the analysis of DJ-1. All three antibodies showed the same low abundance of DJ-1 in cells from homozygous mutation carriers (fig. S1, C and D), and mass spectrometry only detected peptides unique to DJ-1 in the cell lysates of healthy controls (Fig. 1H).

The c.192G>C mutation in the *PARK7* gene causes skipping of exon 3

To further explore the reduced protein amount, we analyzed *PARK7* mRNA expression. We found that *PARK7* RT-PCR (reverse transcription polymerase chain reaction) products of homozygous c.192G>C mutation carriers were shorter than expected and that heterozygous mutation carriers exhibited both a long and a short RT-PCR fragment (Fig. 2A, top). Sequencing of the RT-PCR fragments amplified from control and patient-derived smNPC revealed that exon 3 was skipped in the patient's mRNA (Fig. 2A, bottom). Targeted resequencing of the entire *PARK7* locus in the index patient excluded the presence of other mutations potentially related to the observed aberrant splicing (Fig. 2B and data file S1). Quantitative RT-PCR of RNA from iPSC-derived neurons showed that the overall *PARK7* mRNA amount (including full-length and Δex3 mRNA) was comparable between healthy controls and heterozygous and homozygous mutation carriers (Fig. 3A). However, the amount of full-length *PARK7* mRNA was reduced by half in the heterozygous cells and was almost undetectable in cells derived from homozygous carriers (Fig. 3B). Nevertheless, Δex3 mRNA was indeed as abundant in patient-derived cells as full-length *PARK7* mRNA in control cells, as shown by Northern blot (Fig. 3C).

To test whether the G>C substitution was sufficient to cause exon skipping, we cloned *PARK7* exon 3 and the flanking regions from a healthy donor and from the index patient into the minigene vector pSPL3. We then specifically introduced the c.192G>C mutation into the wild-type (wt) *PARK7* minigene construct and vice versa. Upon expression in human embryonic kidney (HEK) 293 cells, only minigene constructs encoding wt and corrected patient's exon 3 gave rise to full-length complementary DNA (cDNA). Transcripts of both minigene constructs carrying the mutation were aberrantly spliced (Fig. 3D), suggesting that the c.192G>C mutation was sufficient to cause exon skipping. Consistent with these in vitro results, the monoallelic correction of the mutation ex vivo in patient-derived (hom2) fibroblasts by gene editing (fig. S3, A to D) rescued the aberrant splicing of one allele, leading to both full-length and Δex3 mRNA as expected for the heterozygous state (Fig. 3E and fig. S3D). The correction of one allele was sufficient to rescue DJ-1 protein expression in those cells (Fig. 3F). The mutation occurs at the last position of exon 3. Therefore, we predicted that U1-mediated splicing was involved in the pathogenic mechanism related to c.192G>C by creating an additional mismatch that abolishes the binding of U1 snRNA to the splice donor site (fig. S4A).

Genetically engineered U1 snRNA rescues aberrant splicing and loss of protein

We tested our hypothesis by cloning an adapted U1 snRNA (G>C U1 snRNA) to restore binding to c.192G>C mutant pre-mRNA. According to our predictions, G>C U1 snRNA should restore the correct splicing of c.192G>C *PARK7* mRNA (fig. S4B). Exon 3 was skipped in the minigene assay when a *PARK7* construct harboring the c.192G>C exon 3 was cotransfected with wt U1 snRNA, but exon skipping was partially rescued when cells were cotransfected with G>C U1 snRNA (Fig. 4A). This in vitro rescue was next translated into our ex vivo cellular model. smNPCs were stably transduced with either wt U1 snRNA or G>C U1 snRNA expression constructs (fig. S5A). Whereas expression of wt U1 snRNA showed no significant effect ($P > 0.05$), full-length *PARK7* mRNA was significantly ($P \leq 0.01$) increased upon G>C U1 snRNA expression (Fig. 4B). This rescue of full-length mRNA translated into a significant ($P < 0.05$) rescue of DJ-1 protein expression. Compared to control smNPC, untransduced and wt U1 snRNA-transduced clones all showed less than 5% DJ-1 protein (Fig. 4C). Transduction of both clones with G>C U1 snRNA vectors resulted in an increase in DJ-1 protein expression above 10% (Fig. 4C). These smNPCs were further differentiated into neurons (fig. S5, B to D), and the rescue remained stable upon differentiation, with G>C U1 snRNA-expressing neurons showing significantly ($P < 0.05$) increased DJ-1 protein (Fig. 4D).

Impaired translation of c.192G>C mutant mRNA causes loss of DJ-1 protein

Because exon 3 skipping is in frame, a shorter DJ-1 peptide would be expected that lacks 34 amino acids encoded by exon 3. However, no truncated protein could be detected (Fig. 1 and fig. S1, A and C). To exclude that expression of DJ-1 protein in our patient-derived cell model was impaired by defects of the translation machinery unrelated to the mutation itself, we overexpressed wt DJ-1 by lentiviral

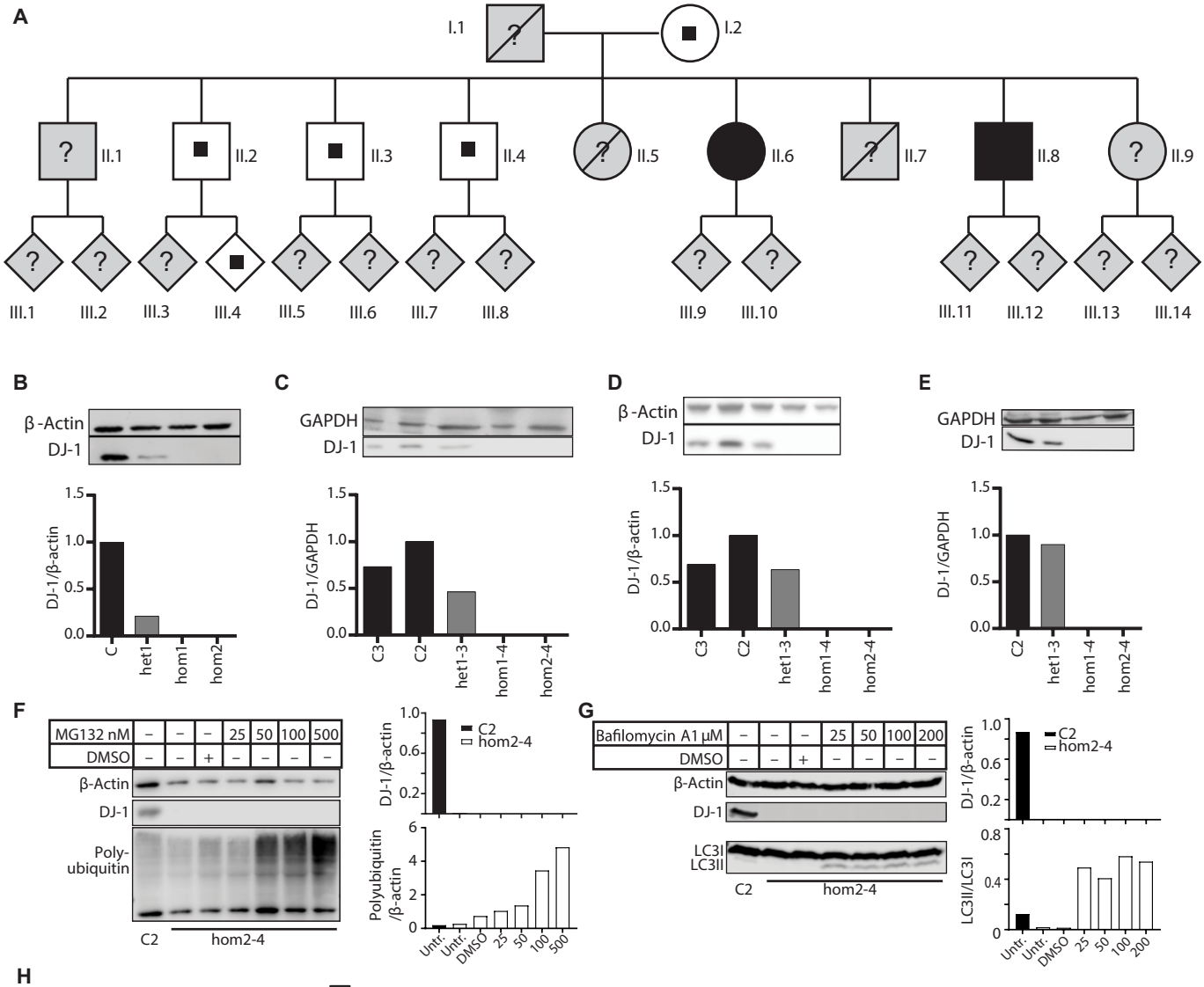

Fig. 1. The c.192G>C *PARK7* mutation leads to pronounced loss of DJ-1 protein in mutation carriers. (**A**) Pedigree structure of the family of c.192G>C mutation carriers. Black symbols denote homozygous carriers. Symbols with a black dot denote heterozygous carriers. White symbols denote healthy individuals, and question marks denote untested individuals. The pedigree has been modified to prevent identification of individuals. (**B** to **E**) Immunoblots and densitometry of DJ-1 and housekeeping proteins in fibroblasts (B), iPSC (C), smNPC (D), and neurons (E). (**F**) Representative immunoblot and densitometry of DJ-1 after blocking of proteasomal degradation in patient-derived smNPC with increasing concentrations of MG132. β-Actin was used as loading control, and detection of increasing polyubiquitination was used as treatment control. $n = 4$ Western blots. (**G**) Representative immunoblot and densitometry of DJ-1 after blocking the autophagy-lysosomal pathway in patient-derived smNPC with increasing concentrations of bafilomycin A1. β-Actin was used as loading control, and the detection of increasing LC3II amount was used as treatment control. $n = 4$ Western blots. (**H**) Number of peptides with a sequence unique for DJ-1 (solid bars, right *y* axis) detected by mass spectrometry and the signal intensity of these measurements calculated as the label-free quantification (LFQ) (striped bars, left *y* axis) in protein lysates of control and patient-derived smNPCs.

transduction of patient-derived smNPC. Moreover, we transduced cells with a Δex3 *PARK7* cDNA vector whose transcript requires no splicing and is expected to translate into a truncated protein (fig. S5E). Overexpression of the wt *PARK7* sequence restored DJ-1 protein expression in clones hom2-1 and hom2-4 (Fig. 5A). However, overexpression of the Δex3 vector failed to increase DJ-1 protein expression (Fig. 5A). In line with this observation, the overexpression of wt *PARK7* resulted in a significant ($P \leq 0.0001$) increase of full-length mRNA (Fig. 5B, left graph). Although the expression of Δex3 mRNA was significantly ($P \leq 0.0001$) increased in transduced clones compared to those of untransduced clones (Fig. 5B, right graph), truncated protein was still not detected (Fig. 5A). This observation was confirmed after neuronal differentiation of those transduced smNPCs (Fig. 5C).

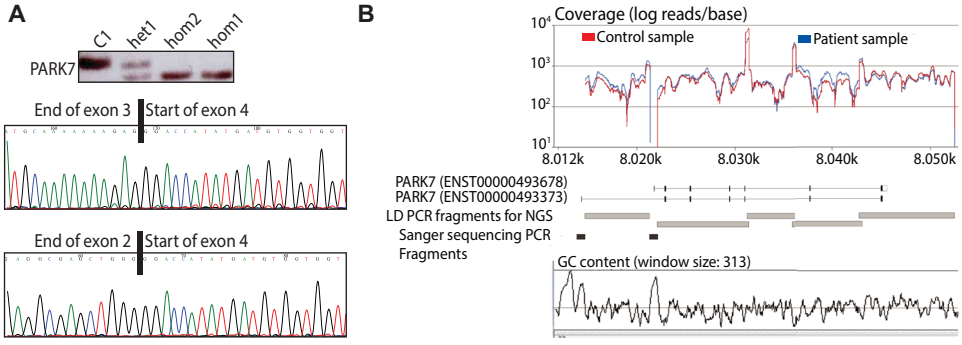

Fig. 2. Targeted resequencing of *PARK7*. (**A**) (Top) Agarose gel visualizing amplification of *PARK7* cDNA derived from the indicated fibroblasts. (Bottom) Segments of electropherograms of Sanger sequencing of *PARK7* cDNA from control (top) and patient-derived (bottom) smNPC showing the bases before and 20 bases of exon 4. (**B**) Targeted resequencing of the *PARK7* gene in the proband ruled out the presence of other mutations potentially related to the observed aberrant splicing. Targeted resequencing was performed by a combination of NGS of overlapping long distance (LD) PCR fragments and Sanger sequencing of two gap closure amplicons for high GC content segments (see GC content plot at the bottom), which cover the entire *PARK7* gene (two main *PARK7* transcripts with alternative first exons depicted in the center). NGS yielded 60,977 and 59,830 target mapped reads for the proband and a parallel-processed control subject; the coverage in log reads/base for both individuals is depicted by the colored graphs in the top diagram; 99.78% (proband) and 99.67% (control) of the sequence targeted by NGS were covered by ≥50 reads. The list of high-confidence variants observed in the proband is provided in data file S1.

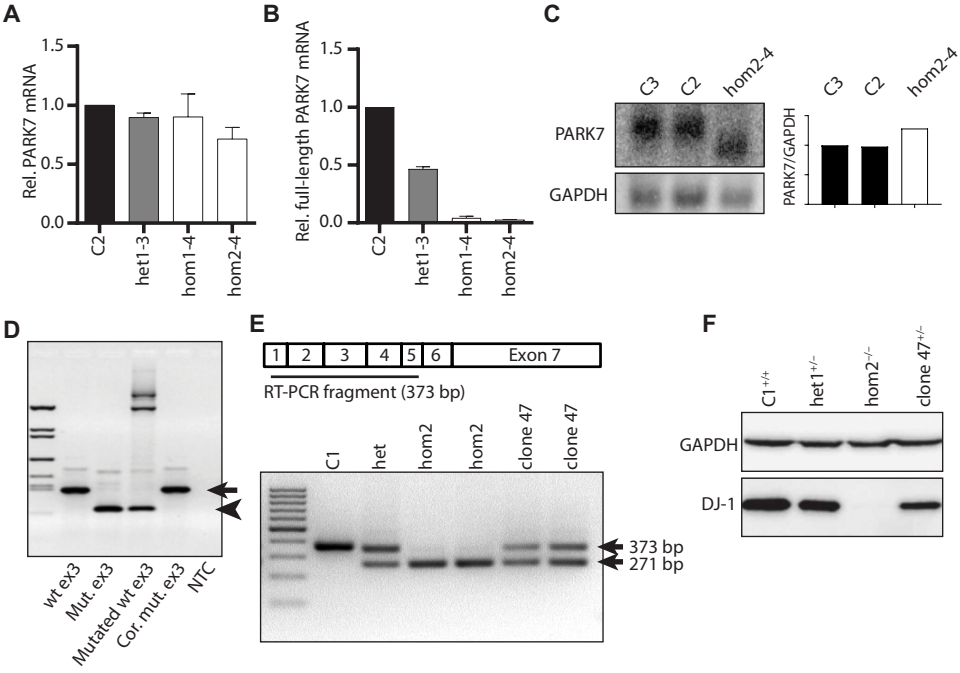

Fig. 3. The c.192G>C *PARK7* mutation causes skipping of exon 3. (**A** and **B**) Assessment of *PARK7* mRNA expression in iPSC-derived neurons by SYBR green qPCR (quantitative PCR) of overall *PARK7* (A) or only full-length *PARK7* (B). Expression was normalized to expression of *ACTB* and *TBP*. Ratios were normalized to control C2 ($n = 3$). Values show means + SEM. (**C**) Northern blot detection and quantification of *PARK7* and *GAPDH* mRNA from total RNA of indicated smNPC. (**D**) Minigene assay showing the effect of wt and c.192G>C *PARK7* exon 3 on splicing. The upper band (arrow) represents cDNA amplicon including exon 3, and the lower band (arrowhead) represents cDNA lacking exon 3. NTC, no template control. (**E**) Isogenic correction of the c.192G>C *PARK7* mutation in immortalized fibroblasts of the index patient. (Top) Schematic image of the amplified RT-PCR fragment. (Bottom) Agarose gel of RT-PCR from two independent RNA extractions of fibroblasts. The 373–base pair (bp) band represents correctly spliced *PARK7* mRNA, and the 271-bp band represents Δex3 *PARK7* mRNA. (**F**) Immunoblot of DJ-1 protein expression before and after gene editing in patient-derived immortalized fibroblasts compared to fibroblasts of control C and heterozygous carrier het1. GAPDH (glyceraldehyde-3-phosphate dehydrogenase) served as loading control.

Next, we investigated the predicted centroid secondary structure of mRNA, where 47.1% of the bases were predicted to be unpaired for wt *PARK7*, whereas only 40.3% were unpaired for the Δex3 variant. This difference in the number of unpaired bases in the native mRNA structure is also reflected by a slightly higher predicted minimum free energy (−271.1 kcal/mol) than that in the Δex3 variant (−273.1 kcal/mol). These energy predictions can only provide indicative estimates, although structure visualizations (Fig. 5D) pointed to systematic differences between the variants across several bases in one specific local branch, between the bases at positions 209 and 486 in the native structure, and between bases 214 and 381 in the mutant. In this secondary structure branch, most of the bases in the native structure were unpaired, whereas the corresponding branch in the mutant was dominated by base pairs forming stem-loop structures. However, the predicted differences in mRNA structure do not result in inhibition of mRNA transport from the nucleus to the cytoplasm where translation takes place. Northern blot analyses of cytosolic and nuclear fractions of smNPC showed no difference in *PARK7* mRNA amounts between control lines and patient-derived cells (Fig. 5E and fig. S6A). To completely exclude an inhibition of the translation by any other cellular mechanism, both vectors, wt and Δex3 *PARK7*, were used for in vitro translation. Whereas the translation of in vitro transcribed wt *PARK7* mRNA led to production of full-length protein, Δex3 mRNA failed to be translated into truncated DJ-1 protein in vitro (Fig. 5F and fig. S6, B and C). Next, we explored whether impaired Δex3 *PARK7* translation is only related to interference with the eukaryotic translation machinery. When expressed in a prokaryotic organism, Δex3 *PARK7* cDNA also failed to be translated (Fig. 5G). *Escherichia coli* transformed with either Δex3 *PARK7* or wt *PARK7* cDNA constructs expressed *PARK7* mRNA (Fig. 5G, top); however, only wt *PARK7* mRNA was translated into protein (Fig. 5G, bottom, and fig. S6D). Together, our results show that the lack of DJ-1 protein in homozygous c.192G>C carriers is not caused by mRNA instability or mislocalization but rather by impaired translation of Δex3 *PARK7* mRNA.

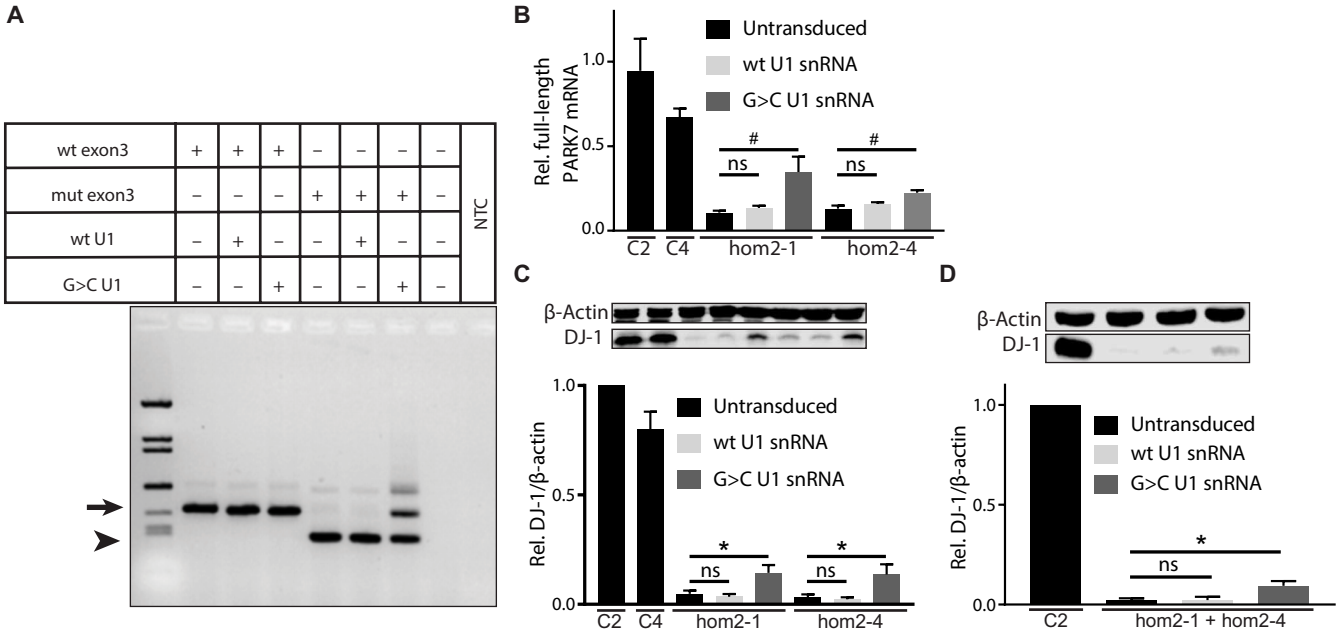

Fig. 4. Genetically engineered U1 snRNA rescues aberrant splicing and loss of protein. (**A**) Minigene assay in HEK293 cells expressing indicated *PARK7* exon 3 constructs cotransfected with indicated U1 snRNA constructs. The upper band (arrow) represents the cDNA amplicon including exon 3, and the lower band (arrowhead) represents Δex3 cDNA. (**B**) Full-length *PARK7* mRNA expression normalized to *ACTB* in indicated smNPC lines after lentiviral transduction. One-step RT-qPCR was performed using TaqMan probes detecting full-length *PARK7* and *ACTB* mRNA. Values show means + SEM. Kruskal-Wallis test followed by Dunn's multiple comparisons test, $n \geq 3$. (**C**) Immunoblot of DJ-1 of indicated, transduced smNPC lines. (Top) Representative Western blot showing β-actin (top) and DJ-1 (bottom). (Bottom) Quantification of DJ-1 protein normalized to β-actin of indicated smNPC lines after lentiviral transduction. Values are normalized to control C2 and show means + SEM. Friedman test followed by Dunn's multiple comparisons test, $n = 5$ to 8. (**D**) Immunoblot of DJ-1 in neurons differentiated in vitro from indicated, transduced smNPC lines. (Top) Representative Western blot showing β-actin (top) and DJ-1 (bottom). (Bottom) Quantification of DJ-1 protein normalized to β-actin. Values are normalized to control C2 and show means + SEM. Friedman test followed by Dunn's multiple comparisons test, $n = 6$. $^{*}P \leq 0.05$, $^{\#}P \leq 0.01$. ns, not significant.

Reintroduction of DJ-1 rescues cellular phenotypes in immortalized fibroblasts

Loss of DJ-1 interferes with mitochondrial function and morphology in cellular models. We previously reported that murine DJ-1 knockout (KO) fibroblasts exhibit reduced mitochondrial membrane potential (MMP) (*17*). Human immortalized fibroblasts hom2-im derived from the index patient showed significantly ($P < 0.0001$) reduced MMP compared to that in healthy control C-im that was significantly ($P \leq 0.0001$) rescued after reintroduction of wt DJ-1 by transfection (Fig. 6A).

Currently, even successful genetic intervention as a rescue strategy cannot be directly translated into a treatment option for patients. Therefore, we performed literature mining for the prioritization of candidate compounds that target U1-dependent mis-splicing and may rescue DJ-1 protein in our patient-based cellular models of PD. The plant cytokinin kinetin (6-furfurylaminopurine) was reported to successfully rescue pathologic exon skipping of *IKBKAP* pre-mRNA in patients with familial dysautonomia (FD) (*18*). Here, we tested the kinetin analog RECTAS (rectifier of aberrant splicing) (*19*), which has been described to be even more potent in cellular models of FD. Because of the limited efficiency of RECTAS to consistently increase full-length *PARK7* mRNA to sufficient and relevant amounts in our cells (fig. S6E), we applied an in-house computational literature mining tool and identified phenylbutyric acid (PB) as a compound that selectively increased *PARK7* mRNA expression in rat dopaminergic N27 cells and human HEK293 cells (*20*). We hypothesized a synergistic effect of RECTAS when combined with PB to rescue DJ-1 in c.192G>C carriers. After a 4-day treatment of hom2-im fibroblasts with 1 mM PB and 10 or 25 μM RECTAS, we observed a dose-dependent increase in DJ-1 protein that reached statistical significance ($P < 0.01$) at the higher concentration (Fig. 6B). This increase was of physiological relevance because it led to an increase in MMP: Whereas untreated and ethanol (EtOH)/dimethyl sulfoxide (DMSO)–treated hom2-im fibroblasts showed decreased MMP compared to that in healthy control C-im, the MMP was significantly ($P < 0.05$) increased in fibroblasts treated with 1 mM PB and 10 μM RECTAS (Fig. 6C).

Pharmacologic treatment of aberrant splicing rescues neuronal cell loss in midbrain organoids

To observe the rescue in a more disease-relevant cell model, we differentiated neurons from two patient-derived smNPC clones (fig. S5C) and treated for 4 days with indicated concentrations. Compared to the untreated and the EtOH/DMSO-treated neurons, correctly spliced full-length *PARK7* mRNA was significantly ($P < 0.05$) increased after treatment with 1 mM PB and 50 μM RECTAS (Fig. 6D, left graph). At the same time, the ratio of full-length mRNA to Δex3 mRNA increased significantly ($P < 0.05$) in treated cells, indicating that the combinatorial treatment not only increased full-length mRNA amounts but also rescued the pathologic exon skipping (Fig. 6D, right graph). Therefore, we chose the concentration of 25 μM and the most effective concentration of 50 μM for longer treatments of 14 days to rescue DJ-1 protein. DJ-1 protein expression increased up to 8.84 and 17.77% compared to the healthy control upon treatment with 1 mM

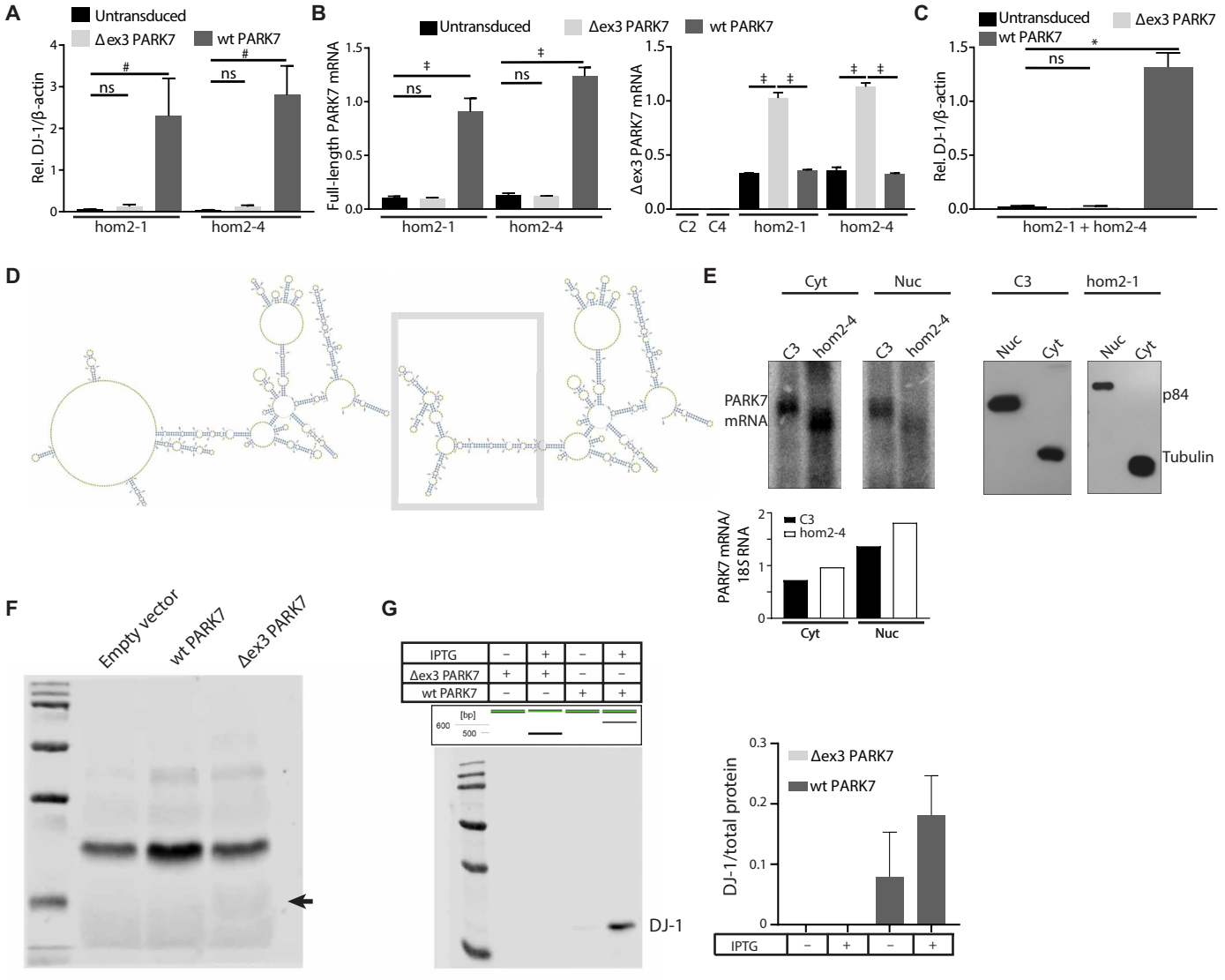

Fig. 5. Mechanism mediating the loss of protein. (**A**) Quantification of DJ-1 immunoblots of indicated, transduced smNPC clones. DJ-1 amount was normalized to β-actin. Values are normalized to control C2 (Fig. 4D) and show means + SEM. Kruskal-Wallis test followed by Dunn's multiple comparisons test, $n = 5$ to 8. (**B**) One-step RT-qPCR results of the indicated smNPC clones. Full-length *PARK7* mRNA (left graph) and Δex3 *PARK7* mRNA (right graph) were detected by duplex one-step RT-qPCR using TaqMan probes and normalized to *ACTB*. Values show means + SEM. One-way ANOVA followed by Holm-Sidak's multiple comparisons test, $n = 3$ to 7. (**C**) Quantification of DJ-1 immunoblots of neurons differentiated in vitro from indicated, transduced smNPC clones. DJ-1 amounts were normalized to β-actin. Values are normalized to control C2 (Fig. 4E) and show means + SEM. Kruskal-Wallis test followed by Dunn's multiple comparisons test, $n = 6$. (**D**) Secondary structure predictions for wt *PARK7* mRNA (left) and Δex3 *PARK7* mRNA (right) were generated using RNAfold software. (**E**) (Left) Northern blot and quantification of the cytosolic (first panel) and nuclear (second panel) fractions of indicated smNPC lines. mRNA was visualized using a *PARK7*-specific probe. (Right) Western blot of the same cytosolic and nuclear fractions of smNPC C3 (third panel) and hom2-4 (fourth panel) stained with anti-p84 and anti-tubulin antibodies to confirm the purity of the fractions. (**F**) Immunoblot of in vitro translation of *PARK7* mRNA that was transcribed in vitro from empty vector, wt *PARK7* vector, or Δex3 *PARK7* vector. The arrow indicates the expected size of a Δex3 DJ-1 protein. Representative image out of four independent experiments. (**G**) Expression of recombinant DJ-1 in *E. coli* BL21 after transformation with wt *PARK7* or Δex3 *PARK7* plasmids. Representative figure of *PARK7* cDNA amplification from bacterial RNA without and with induction of plasmid expression by isopropyl-β-D-thiogalactopyranoside (IPTG) (top), and immunoblot of DJ-1 protein and quantification ($n = 2$) from respective bacterial lysates (bottom). $^{*}P \leq 0.05$, $^{\#}P \leq 0.01$, and $^{\ddagger}P \leq 0.0001$.

PB and 25 or 50 μM RECTAS, respectively, whereas EtOH/DMSO treatment showed no increase (Fig. 6E). This rescue of aberrant splicing in patient-derived neurons carrying the c.192G>C mutation translates into full-length mutant p.E64D DJ-1 protein. Studies with recombinant p.E64D DJ-1 revealed no severe cellular phenotype caused by the mutation and only subtle effects on protein stability (*11*, *13*, *14*). Therefore, we hypothesized that the translation of c.192G>C mutant mRNA (encoding p.E64D DJ-1 protein) in human neuronal cells would still compensate for the loss of DJ-1 and at least partly restore physiological DJ-1 function.

To analyze whether mutant DJ-1 induces a disease-related phenotype in a more physiological relevant in vitro model, we generated isogenic midbrain-specific organoids that were derived from the control line C4 and the isogenic line C4Mut, in which the pathogenic c.192G>C mutation was inserted via CRISPR-Cas9 technology. smNPC spheroids were generated, kept in maintenance medium for 10 days,

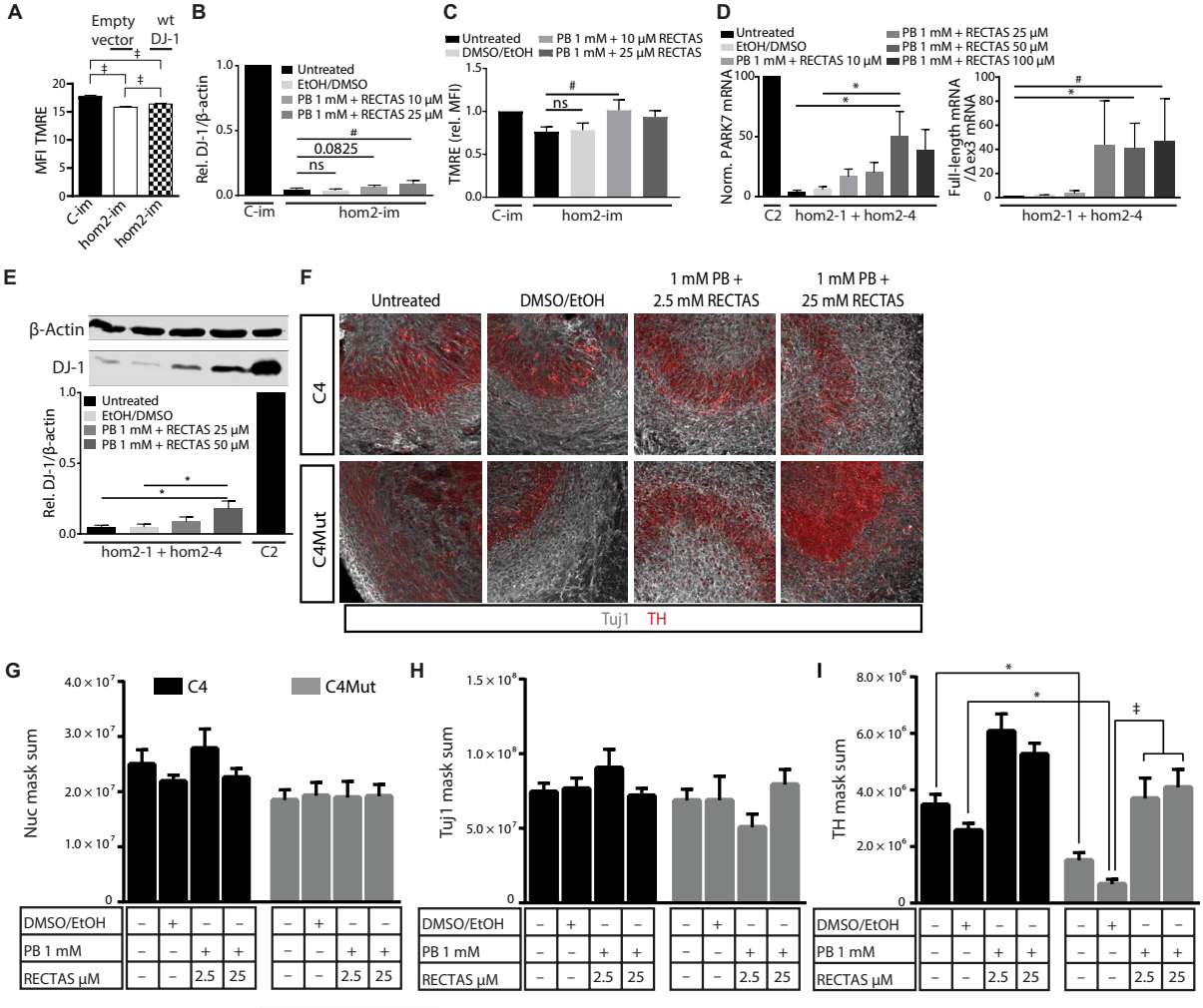

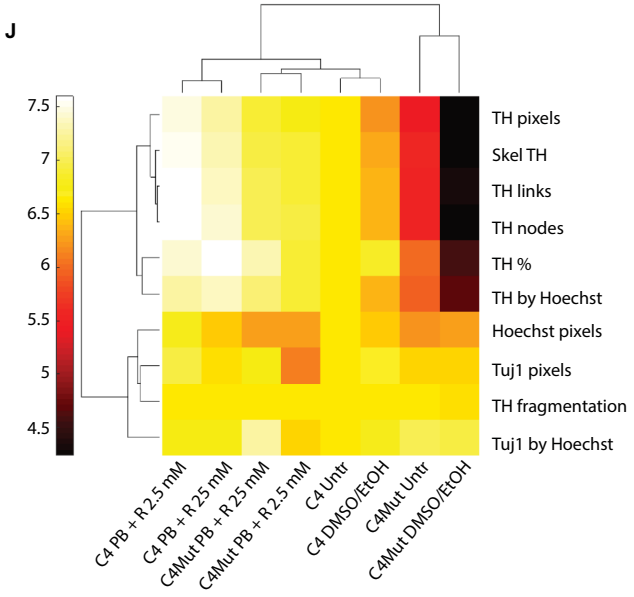

Fig. 6. Genetic and pharmacologic rescue of loss of DJ-1–related cellular phenotypes. (**A**) MMP quantification represented as mean fluorescence intensity (MFI) of the tetramethylrhodamine, ethyl ester (TMRE) signal of indicated lines. Values show means + SEM. $n = 3$. Kruskal-Wallis test followed by Dunn's multiple comparisons test. (**B**) Densitometry of DJ-1 immunoblots of indicated immortalized fibroblast lines after 4 days of treatment. DJ-1 was normalized to β-actin. Values are normalized to control C-im and show means + SEM. Friedman test followed by Dunn's multiple comparisons test, $n = 5$. (**C**) Flow cytometric analysis of MMP by TMRE staining in indicated immortalized fibroblast lines after 4 days of treatment compared to untreated lines (black bars). Values are normalized to control C-im and show means + SEM. Friedman test followed by Dunn's multiple comparisons test, $n = 7$. (**D**) Amounts of correctly spliced full-length *PARK7* mRNA (left graph) and ratio of full-length to Δex3 mRNA in in vitro differentiated neurons after 4 days of treatment as determined by duplex TaqMan RT-qPCR. Full-length and Δex3 *PARK7* mRNA expression was normalized to expression of *ACTB*. Values are normalized to control C2 (left graph) or to the untreated patient-derived neurons (right graph) and show means + SEM. One-way ANOVA followed by Tukey's multiple comparisons test (left graph), $n = 5$ to 8, and Kruskal-Wallis test followed by Dunn's multiple comparisons test (right graph), $n = 4$ to 7. (**E**) (Top) Representative immunoblot of DJ-1 and β-actin of in vitro differentiated neurons from indicated clones treated for 14 days. (Bottom) Quantification of DJ-1 normalized to β-actin. Values are normalized to control C2 and show means + SEM. One-way ANOVA followed by Holm-Sidak's multiple comparisons test, $n = 3$ to 5. (**F**) Representative maximum intensity projection of confocal images of C4 and C4Mut midbrain organoids, showing Tuj1 and TH staining. (**G** to **I**) Bar graphs showing quantification of Hoechst$^+$ (G), Tuj1$^+$ (H), and TH$^+$ (I) pixels in untreated or treated C4 and C4Mut midbrain organoids. Bars represent means + SEM. One-way ANOVA followed by Turkey's multiple comparisons test. The midbrain organoid derivation was performed three times (total number of sections analyzed: C5 Untr, 13; C5 Veh, 16; C5 PB 1 mM PB + RECTAS 2.5 μM, 9; C5 PB 1 mM PB + RECTAS 25 μM, 12; C5 Mut, 16; C5Mut Veh, 17; C5 PB 1 mM PB + RECTAS 2.5 μM, 13; C5 PB 1 mM PB + RECTAS 25 μM, 13. (**J**) Heatmap and cluster analysis of all the features extracted from the image analysis of treated midbrain organoids. $^*P < 0.05$, $^\#P \leq 0.01$, and $^\ddagger P \leq 0.0001$.

and subsequently differentiated into midbrain-specific organoids and treated with PB and RECTAS, at indicated concentrations, until day 35, for a total duration of 25 days. No difference was observed between C4 and C4Mut organoids in terms of number of overall cells and neurons specifically, as detected by staining with Hoechst and Tuj1 staining, respectively (Fig. 6, F, left column, G, and H). However, the number of TH^+ (tyrosine hydroxylase–positive)–dopaminergic neurons was markedly decreased in C4Mut organoids. This specific dopaminergic phenotype of loss of DJ-1 in human midbrain organoids was rescued in a dose-dependent manner by the administration of 1 mM PB and 2.5 or 25 μM RECTAS (Fig. 6, F and I). A high-level view of all features extracted from the image analysis (table S1) shows distinct clustering of untreated and EtOH/DMSO-treated C4Mut organoids (Fig. 6J). After treatment with PB and RECTAS, C4Mut organoids cluster together with the organoids generated from the wt line C4 (Fig. 6J).

Sporadic PD cases have a higher burden of harboring deleterious splice variants

Mutations in *PARK7* are a rare cause of PD, and the c.192G>C mutation was found in a single family of Turkish descent until now. However, splice-site mutations are common in humans with about 30% of all mutations causing aberrant splicing (*12*, *21*). To determine whether mutations in U1-binding sites might play a role in the common sporadic form of PD, we performed a burden analysis of next-generation sequencing (NGS) data from PD cases (fig. S7). We first used the whole-exome sequencing (WES) data from the Parkinson's Progression Markers Initiative (PPMI) study (www.ppmi-info.org). After sample processing and quality control (QC), we compared 372 PD and 161 control sequences. We observed a significant burden for genome-wide mutations in U1-binding sites in cases compared to the controls [$P = 0.012$, odds ratio (OR) = 1.39, confidence interval (CI) = 1.08 to 1.82]. The signal was coming mainly from exonic variants in 5′ splicing sites ($P = 0.028$, OR = 1.37, CI = 1.04 to 1.84). To increase the statistical power of the test and further test the hypothesis of a higher burden in typical PD, we subsequently repeated our analysis in a larger cohort for PD exomes. From the sequencing data of the ongoing Parkinson Disease Genome Sequencing Consortium (PDGSC) project, we analyzed sequencing data from 2710 PD cases and 5713 controls. In both cohorts, the control datasets were age- and sex-matched with the corresponding patient cohorts. Individuals with neurological dysfunctions were excluded from the control cohorts. The burden analysis of this replication cohort confirmed the higher burden of splice-site mutations in typical PD cases compared to controls with an FDR (false discovery rate) adjusted *P* value of 0.014 ($P = 0.007$, OR = 1.04, CI = 1.01 to 1.08, *P* value FDR adjusted = 0.014). Similar to the PPMI cohort, the signal was mainly driven by exonic splice-site variants ($P = 0.003$, OR = 1.11, CI = 1.03 to 1.19, *P* value FDR adjusted = 0.011), and within this group of genes, the main signal is driven by variants in brain-expressed genes with an FDR-adjusted *P* value of <0.0001 (Fig. 7, right). (See data file S2 for a list of brain-expressed genes harboring variants uniquely identified in cases from both cohorts.)

DISCUSSION

Here, we describe a mechanistic concept for the pathogenesis of PD related to U1 splice-site mutations that was identified and validated on the basis of the previously reported PD-associated c.192G>C mutation in *PARK7* (*11*). In contrast to a missense mutation predicted to cause instability of E64D mutant DJ-1 protein, we identified a drastic reduction of DJ-1 protein in patient-based cellular models due to U1-dependent mis-splicing of pre-mRNA. These results are in line with a recent study showing that about 10% of pathogenic missense variants predicted to alter protein coding essentially disrupt splicing (*12*). The demonstration of the disease-causing Δex3 *PARK7* mRNA splice variant as a cause of the drastically reduced expression of DJ-1 protein reported here underscores the relevance of access to patient material for functional studies to validate predictions and define the underlying molecular pathology. Together with the demonstration of an overrepresentation of mutations in U1 splice sites as a more general feature in sporadic cases of PD, our study provides the basis for precision medicine approaches in PD.

The observed discrepancy between the overall amount of mutant pre-mRNA and the drastically reduced amounts of DJ-1 protein in homozygous c.192G>C carriers indicated the involvement of pathological mRNA processing and/or translation and argued against nonsense-mediated decay (NMD) as the underlying mechanism (*22*–*24*). To confirm a U1-mediated pathogenic splicing mechanism underlying the loss of DJ-1 function in PD, we performed genetic rescue experiments. Genetically engineered U1 snRNAs have been shown to partially restore correct splicing using artificial splicing reporter assays in established cell lines in vitro (*25*). This approach may open avenues for future gene transfer strategies for the central nervous system, as options for viral vectors delivered to the brain are becoming safer and more effective (*26*). Currently, however, pharmacological treatment remains the most straightforward strategy to translate our findings into neuroprotective treatment options.

Here, we successfully applied an advanced literature mining approach for the prioritization of candidate drugs to revert molecular and cellular phenotypes. The combination of a compound rectifying aberrant splicing in FD (*19*) with an enhancer of DJ-1 expression (*20*) increased the mRNA and protein amounts of DJ-1 in patient-based cells across different cell types. No complete rescue of protein expression to control was required to restore mitochondrial function. Three-dimensional (3D) self-organizing organoids (*27*) recapitulate the spatial architecture, multilineage differentiation, and cell-cell interactions of the original tissue (*28*, *29*). To investigate the specific effect of the mutation and to eliminate effects caused by different genetic backgrounds, we generated isogenic midbrain-specific organoids. The restitution of dopaminergic integrity and related neuronal features of treated C4Mut organoids were comparable to organoids of the wt line C4 and, hence, segregate together in the cluster analysis. DJ-1 KO mice do not display changes of the integrity of dopaminergic neurons in the substantia nigra compared to wt littermates (*30*, *31*). We believe that the human-specific phenotype in 3D cultures of midbrain organoids adds to the observation that the higher dopamine metabolism observed in human neurons compared to mice contributes to the selective vulnerability of these neurons (*32*).

Our findings regarding a causative treatment for DJ-1 deficiency have an immediate impact for homozygous carriers of the c.192G>C mutation, and this strategy may qualify as treatment at the prodromal stage of PD for addressing neuroprotective strategies in PD (*33*). PB is a U.S. Food and Drug Administration–approved compound used as adjunctive therapy in the management of patients with urea cycle disorders (*34*). As a histone deacetylase inhibitor, PB is thought to

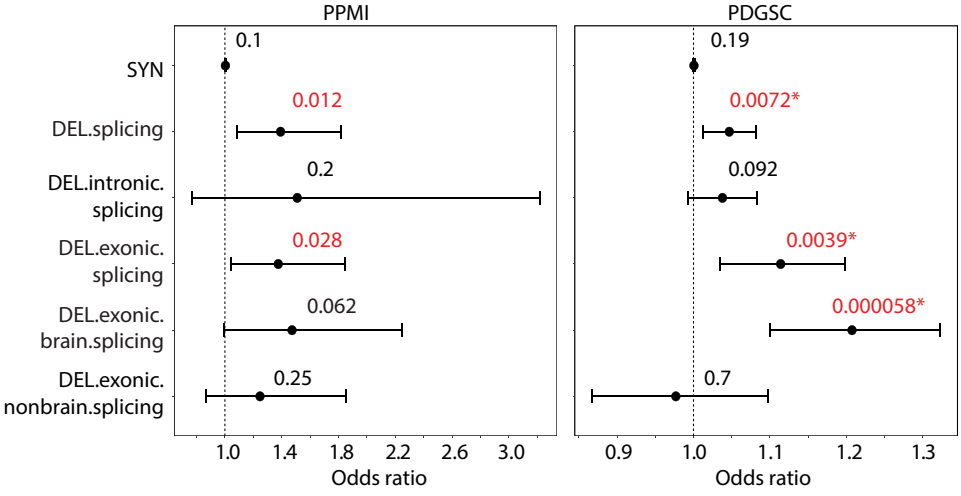

Fig. 7. Burden analysis of splice-site variants in sporadic PD cases. A forest plot representing the burden analysis across different variant classes. Each dot represents the OR, and the value on top of each dot represents the corresponding uncorrected *P* value. Values in red indicate nominal significant *P* values; * indicates FDR-adjusted *P* values of <0.05. (**Left**) Results of the PPMI discovery cohort analysis (the upper limit of CI in the plot is restricted to the maximum of ORs). (**Right**) Results for the PDGSC replication cohort. SYN, rare and low-frequency synonymous variants; DEL.splicing, deleterious splicing variants; DEL.intronic.splicing, deleterious variants in intronic regions; DEL.exonic.splicing, deleterious variants in coding regions; DEL.exonic.brain.splicing, DEL.exonic.splicing variants present in genes expressed in the brain; DEL.exonic.nonbrain.splicing, DEL.exonic.splicing variants present in genes that are not expressed in the brain.

increase DJ-1 expression via increased binding of Sp1 to the *PARK7* promoter (*20*, *35*). Earlier studies have described a neuroprotective role for PB in PD models of pathological aggregation of α-synuclein, although these reports did not account for its effect via DJ-1 up-regulation (*36*, *37*). Loss of DJ-1 protein in *PARK7*-linked PD causes pathological α-synuclein aggregation in the brains of patients, thereby defining synucleinopathy (*38*). For RECTAS, rapid absorption after oral administration, subsequent stability in plasma, and the detection of relevant doses of the compound in the brain after blood-brain barrier penetration were shown (*19*). Moreover, transcriptomic analyses revealed a high specificity of RECTAS, only affecting splicing of a limited set of genes (*19*). As a first drug candidate for the correction of aberrant splicing, kinetin recently underwent clinical assessments for pharmacokinetics, safety, and effectiveness in vivo (*39*, *40*). In a clinical trial, kinetin was well tolerated and safe and resulted in increased expression of correctly spliced mRNA in vivo (*39*). This finding indicates that drugs targeting U1-mediated splicing defects have great potential to become therapeutic tools and supports future clinical trials.

The therapeutic potential of the treatment for targeting defective splicing is further substantiated by additional mutations in monogenic PD. Homozygous mutations in *PARK7* affecting the 5′ consensus splice site for U1 were described as a c.91-2AG mutation in an Iranian family and a c.317-322del mutation in a Turkish family (*8*, *9*). Moreover, the c.1488+1 G>A mutation in the *PINK1* gene was shown to affect a U1-binding site and cause an in-frame deletion of exon 7 (*6*). As for the c.192G>C mutation in *PARK7*, no NMD of the mutant PINK1 mRNA was observed in affected carriers.

Our findings suggest that the pathogenic relevance of exonic splicing mutations has been underestimated in PD. Although defective pre-mRNA processing is known to represent a common cause of human diseases, with ~30% of all mutations causing aberrant splicing (*12*, *21*), for PD pathogenesis, the dysregulation of splicing as an alternative mechanism contributing to the neurodegenerative process was not systematically addressed (*41*). Our data indicate an enrichment of disease-associated variants also in sporadic PD and underscore the therapeutic potential of compounds acting on pathological splicing.

Despite this potential impact of our findings in sporadic PD that goes beyond the initial rare mutation found in rare familial PD, we need to acknowledge that our study has some limitations. Although the presented combinatorial treatment rescued cellular phenotypes in different experimental models, including iPSC-based midbrain organoids as a complex in vitro model, these results need to be further validated in vivo. Here, rodent models of aberrant DJ-1 splicing may help to test the combinatorial treatment in vivo, not only to validate the rescue of aberrant splicing but also to analyze the efficacy of the compounds at different concentrations as defined by the capacity to cross the blood-brain barrier. Furthermore, the effect of RECTAS cannot be easily predicted for every splice-site donor mutation. RECTAS activity was suggested to depend on auxiliary factors such as hnRNPA1 and therefore acted only on a minor fraction of the human exons in cells derived from a patient with FD (*19*). Because the exact molecular mechanism by which RECTAS restores the inclusion of specific exons (*19*) remains still unknown, the rescuing effect of RECTAS on other mutations needs to be validated on a case-by-case basis. However, our burden analysis in PD cohorts suggest a high prevalence of splice-site donor mutations in brain-expressed genes in PD patients compared to controls from European ancestry. Therefore, a large number of candidate exons can still be expected, which remain to be experimentally validated.

Our study illustrates the promise for treatment approaches in precision medicine in PD that focus on genetic and molecular stratification. To account for the increasingly recognized heterogeneity in PD and other neurodegenerative disorders, additional strategies need to be developed for the stratification of patients along shared pathogenic mechanisms. The candidate drugs identified in our cellular models may translate into basket studies referring to patients sharing the same underlying mechanism, as already shown for precision medicine approaches in cancer, and might allow for clinical trials in patients across groups that share certain molecular signatures (*42*).

MATERIALS AND METHODS

Study design

The objective of this study was to generate patient-derived cellular models to characterize the pathogenic effects of the mutation in *PARK7* that was known by that time as amino acid substitution E64D. After obtaining skin fibroblasts from the index patient and additional family members and reprogramming these into iPSC, we

uncovered that the mutation leads to loss of protein due to aberrant splicing. Because the mutation occurs within the 5′ splice-site donor, we followed different strategies to test the hypothesis that the point mutation causes exon skipping by abolishing the binding of the small nuclear ribonucleoprotein (snRNP) U1. First, we confirmed in vitro by minigene assay and ex vivo by gene editing that the mutation alone is sufficient to cause exon skipping. Subsequently, we applied successfully a genetically engineered U1 snRNA, whose sequence matched the mutated *PARK7* sequence, to restore exon inclusion in vitro and ex vivo. Having deciphered the molecular mechanism by which the mutation causes loss of protein, we used literature mining to identify candidate compounds for pharmacological intervention. After identifying that the combinatorial treatment with PB and RECTAS recues partially exon inclusion and protein expression, we investigated whether the degree of rescue was of biological relevance. Subsequently, we tested the effect of the treatment on the well-established phenotype of impaired MMP in patient-derived fibroblasts, which led us to study the effect of the treatment on midbrain-specific organoids. To eliminate any interference by the genetic background of the patient, we generated an isogenic control iPSC line and revealed a loss of dopaminergic neurons in mutant organoids that was rescued by the treatment. Randomization and blinding were not applied to these in vitro studies, and the number of replications of each experiment can be found in the figure legends. Although mutations in *PARK7* are a rare event, generally, mutations causing aberrant splicing are contributing up to one-third of disease-causing mutations. Therefore, we performed a burden analysis on the WES dataset of the PPMI cohort and detected a higher burden in PD patients. To confirm this result and to gain statistical power, we subsequently analyzed the dataset of the PDGSC cohort, which contains substantially more genetic datasets. The study size was determined by the size of the two cohorts and the filtering we applied. Briefly, cohorts were filtered for European ancestry, and population outliers were removed during QC. For the control groups of both cohorts, individuals with substantial neurological dysfunction were excluded. GenomeAnalysisToolkit (GATK) hard filtering was used to select high-quality single-nucleotide variants (SNVs) with a call rate of >0.9 (PPMI) or >0.8 (PDGSC). Deleterious variants were identified on the basis of the MaxEntScan method and two ensemble scores (*dbscSNV_ADA* and *dbscSNV_RF*), and burden analysis was conducted by constructing a generalized linear model.

Burden analysis

WES data of 372 PD and 161 control samples from the PPMI study were used in the discovery cohort, whereas the replication cohort (PDGSC) was composed of 2710 cases and 5713 controls. The PPMI controls were selected on the basis of the following criteria: (i) 30 years or older, (ii) no first-degree blood relative with PD, (iii) no neurological dysfunction, and (iv) no cognitive impairment based on a Montreal Cognitive Assessment (MoCA) score >26. The controls used in the PDGSC cohort are obtained from a subset of samples from the International Parkinson Disease Consortium (https://pdgenetics.org/about). It is a multicentric consortium consisting of samples obtained from various countries forming the International Parkinson's Disease Genomics Consortium (IPDGC). The following criteria were used to select the controls: (i) mean age at the time of examination of ~50 years (across all the studies) and (ii) were required to have no neurological dysfunction. Briefly, the deleterious U1 splice-site variants were identified on the basis of the MaxEntScan (*43*) method and two ensemble scores (*dbscSNV_ADA* and *dbscSNV_RF*) that are generated from multiple splice-site prediction tools (*44*), which are available as part of the dbNSFP database (*45*). Burden analyses at the whole-exome levels were conducted by constructing generalized linear models (glm) while adjusting for different covariates. For detailed data description and processing, please see Supplementary Materials and Methods.

Statistical analysis

All experimental data represent means ± SEM and were statistically analyzed by one-way analysis of variance (ANOVA) whenever data passed normality test and by Kruskal-Wallis or Friedman test for nonparametric data followed by appropriate post hoc analysis using GraphPad Prism 8.4.0. The value of significance level alpha was set to 0.05. Statistical parameters of each experiment are stated in the figure legends. Burden analysis was performed by constructing generalized linear regression models using R version 3.4.1 while correcting for various confounding factors as described in Materials and Methods. *P* values were adjusted for multiple testing by the function "p.adjust" (R version 3.4.1) using the FDR method.

SUPPLEMENTARY MATERIALS

stm.sciencemag.org/cgi/content/full/12/560/eaau3960/DC1
Materials and Methods
Additional authors note
Fig. S1. Loss of DJ-1 protein in homozygous c.192G>C mutation carriers.
Fig. S2. Characterization of iPSC and smNPC.
Fig. S3. Generation of gene-corrected fibroblasts.
Fig. S4. Schematic of genetic intervention to rescue aberrant splicing of c.192G>C PARK7.
Fig. S5. Transduction and differentiation of smNPC.
Fig. S6. Loading controls from Fig. 5 and RECTAS single treatment.
Fig. S7. Determination of cutoffs for wild_score and maxentscan_change.
Fig. S8. Western blots.
Table S1. Features of midbrain organoids extracted from image analysis.
Table S2. List of primers used for determination of gene expression by CYBR green qPCR.
Table S3. Hydrolysis probes and primers.
Data file S1. High-confidence sequence variants in the proband as determined by resequencing of the PARK7 gene.
Data file S2. List of brain-expressed genes harboring variants uniquely identified in cases from both cohorts.
Data file S3. Raw data.
References (*46–79*)

View/request a protocol for this paper from *Bio-protocol*.

REFERENCES AND NOTES

1. S. Przedborski, The two-century journey of Parkinson disease research. *Nat. Rev. Neurosci.* **18**, 251–259 (2017).
2. A. J. Espay, M. A. Schwarzschild, C. M. Tanner, H. H. Fernandez, D. K. Simon, J. B. Leverenz, A. Merola, A. Chen-Plotkin, P. Brundin, M. A. Kauffman, R. Erro, K. Kieburtz, D. Woo, E. A. Macklin, D. G. Standaert, A. E. Lang, Biomarker-driven phenotyping in Parkinson's disease: A translational missing link in disease-modifying clinical trials. *Mov. Disord.* **32**, 319–324 (2017).
3. R. Krüger, J. Klucken, D. Weiss, L. Tönges, P. Kolber, S. Unterecker, M. Lorrain, H. Baas, T. Müller, P. Riederer, Classification of advanced stages of Parkinson's disease: Translation into stratified treatments. *J. Neural Transm.* **124**, 1015–1027 (2017).
4. P. M. A. Antony, N. J. Diederich, R. Krüger, R. Balling, The hallmarks of Parkinson's disease. *FEBS J.* **280**, 5981–5993 (2013).
5. B. Cholerton, E. B. Larson, J. F. Quinn, C. P. Zabetian, I. F. Mata, C. D. Keene, M. Flanagan, P. K. Crane, T. J. Grabowski, K. S. Montine, T. J. Montine, Precision medicine: Clarity for the complexity of dementia. *Am. J. Pathol.* **186**, 500–506 (2016).
6. L. Samaranch, O. Lorenzo-Betancor, J. M. Arbelo, I. Ferrer, E. Lorenzo, J. Irigoyen, M. A. Pastor, C. Marrero, C. Isla, J. Herrera-Henriquez, P. Pastor, *PINK1*-linked parkinsonism is associated with Lewy body pathology. *Brain* **133**, 1128–1142 (2010).
7. R. Asselta, V. Rimoldi, C. Siri, R. Cilia, I. Guella, S. Tesei, G. Soldà, G. Pezzoli, S. Duga, S. Goldwurm, Glucocerebrosidase mutations in primary parkinsonism. *Park. Relat. Disord.* **20**, 1215–1220 (2014).

8. J. M. Bras, R. J. Guerreiro, J. T. H. Teo, L. Darwent, J. Vaughan, S. Molloy, J. Hardy, S. A. Schneider, Atypical Parkinsonism-Dystonia syndrome caused by a novel DJ1 mutation. *Mov. Disord. Clin. Pract.* **1**, 45–49 (2014).
9. F. Ghazavi, Z. Fazlali, S. S. Banihosseini, S. R. Hosseini, M. H. Kazemi, S. Shojaee, K. Parsa, H. Sadeghi, F. Sina, M. Rohani, G. A. Shahidi, N. Ghaemi, M. Ronaghi, E. Elahi, PRKN, DJ-1, and PINK1 screening identifies novel splice site mutation in PRKN and two novel DJ-1 mutations. *Mov. Disord.* **26**, 80–89 (2011).
10. V. Bonifati, P. Rizzu, F. Squitieri, E. Krieger, N. Vanacore, J. C. van Swieten, A. Brice, C. M. van Duijn, B. Oostra, G. Meco, P. Heutink, DJ-1(PARK7), a novel gene for autosomal recessive, early onset parkinsonism. *Neurol. Sci.* **24**, 159–160 (2003).
11. R. Hering, K. M. Strauss, X. Tao, A. Bauer, D. Woitalla, E.-M. Mietz, S. Petrovic, P. Bauer, W. Schaible, T. Müller, L. Schöls, C. Klein, D. Berg, P. T. Meyer, J. B. Schulz, B. Wollnik, L. Tong, R. Krüger, O. Riess, Novel homozygous p.E64D mutation in DJ1 in early onset Parkinson disease (PARK7). *Hum. Mutat.* **24**, 321–329 (2004).
12. R. Soemedi, K. J. Cygan, C. L. Rhine, J. Wang, C. Bulacan, J. Yang, P. Bayrak-Toydemir, J. McDonald, W. G. Fairbrother, Pathogenic variants that alter protein code often disrupt splicing. *Nat. Genet.* **49**, 848–855 (2017).
13. K. Görner, E. Holtorf, S. Odoy, B. Nuscher, A. Yamamoto, J. T. Regula, K. Beyer, C. Haass, P. J. Kahle, Differential effects of Parkinson's disease-associated mutations on stability and folding of DJ-1. *J. Biol. Chem.* **279**, 6943–6951 (2004).
14. J. D. Hulleman, H. Mirzaei, E. Guigard, K. L. Taylor, S. S. Ray, C. M. Kay, F. E. Regnier, J. C. Rochet, Destabilization of DJ-1 by familial substitution and oxidative modifications: Implications for Parkinson's disease. *Biochemistry* **46**, 5776–5789 (2007).
15. P. Reinhardt, P. Reinhardt, M. Glatza, K. Hemmer, Y. Tsytsyura, C. S. Thiel, S. Höing, S. Moritz, J. A. Parga, L. Wagner, J. M. Bruder, G. Wu, B. Schmid, A. Röpke, J. Klingauf, J. C. Schwamborn, T. Gasser, H. R. Schöler, J. Sterneckert, Derivation and expansion using only small molecules of human neural progenitors for neurodegenerative disease modeling. *PLOS ONE* **8**, e59252 (2013).
16. D. C. Schöndorf, M. Aureli, F. E. McAllister, C. J. Hindley, F. Mayer, B. Schmid, S. P. Sardi, M. Valsecchi, S. Hoffmann, L. K. Schwarz, U. Hedrich, D. Berg, L. S. Shihabuddin, J. Hu, J. Pruszak, S. P. Gygi, S. Sonnino, T. Gasser, M. Deleidi, iPSC-derived neurons from GBA1-associated Parkinson's disease patients show autophagic defects and impaired calcium homeostasis. *Nat. Commun.* **5**, 4028 (2014).
17. G. Krebiehl, S. Ruckerbauer, L. F. Burbulla, N. Kieper, B. Maurer, J. Waak, H. Wolburg, Z. Gizatullina, F. N. Gellerich, D. Woitalla, O. Riess, P. J. Kahle, T. Proikas-Cezanne, R. Krüger, Reduced basal autophagy and impaired mitochondrial dynamics due to loss of Parkinson's disease-associated protein DJ-1. *PLOS ONE* **5**, e9367 (2010).
18. S. A. Slaugenhaupt, J. Mull, M. Leyne, M. P. Cuajungco, S. P. Gill, M. M. Hims, F. Quintero, F. B. Axelrod, J. F. Gusella, Rescue of a human mRNA splicing defect by the plant cytokinin kinetin. *Hum. Mol. Genet.* **13**, 429–436 (2004).
19. M. Yoshida, N. Kataoka, K. Miyauchi, K. Ohe, K. Iida, S. Yoshida, T. Nojima, Y. Okuno, H. Onogi, T. Usui, A. Takeuchi, T. Hosoya, T. Suzuki, M. Hagiwara, Rectifier of aberrant mRNA splicing recovers tRNA modification in familial dysautonomia. *Proc. Natl. Acad. Sci. U.S.A.* **112**, 2764–2769 (2015).
20. W. Zhou, K. Bercury, J. Cummiskey, N. Luong, J. Lebin, C. R. Freed, Phenylbutyrate up-regulates the DJ-1 protein and protects neurons in cell culture and in animal models of Parkinson disease. *J. Biol. Chem.* **286**, 14941–14951 (2011).
21. K. H. Lim, L. Ferraris, M. E. Filloux, B. J. Raphael, W. G. Fairbrother, Using positional distribution to identify splicing elements and predict pre-mRNA processing defects in human genes. *Proc. Natl. Acad. Sci.* **108**, 11093–11098 (2011).
22. A. Freischmidt, K. Müller, A. C. Ludolph, J. H. Weishaupt, P. M. Andersen, Association of mutations in *TBK1* with sporadic and familial amyotrophic lateral sclerosis and frontotemporal dementia. *JAMA Neurol.* **74**, 110–113 (2017).
23. K. Yap, E. V. Makeyev, Regulation of gene expression in mammalian nervous system through alternative pre-mRNA splicing coupled with RNA quality control mechanisms. *Mol. Cell. Neurosci.* **56**, 420–428 (2013).
24. F. Lejeune, Nonsense-mediated mRNA decay at the crossroads of many cellular pathways. *BMB Rep.* **50**, 175–185 (2017).
25. L. Hartmann, K. Neveling, S. Borkens, H. Schneider, M. Freund, E. Grassman, S. Theiss, A. Wawer, S. Burdach, A. D. Auerbach, D. Schindler, H. Hanenberg, H. Schaal, Correct mRNA processing at a mutant TT splice donor in *FANCC* ameliorates the clinical phenotype in patients and is enhanced by delivery of suppressor U1 snRNAs. *Am. J. Hum. Genet.* **87**, 480–493 (2010).
26. B. Kantor, T. McCown, P. Leone, S. J. Gray, Clinical applications involving CNS gene transfer. *Adv. Genet.* **87**, 71–124 (2014).
27. A. S. Monzel, L. M. Smits, K. Hemmer, S. Hachi, E. L. Moreno, T. van Wuellen, J. Jarazo, J. Walter, I. Brüggemann, I. Boussaad, E. Berger, R. M. T. Fleming, S. Bolognin, J. C. Schwamborn, Derivation of human midbrain-specific organoids from neuroepithelial stem cells. *Stem Cell Rep.* **8**, 1144–1154 (2017).
28. D. Dutta, I. Heo, H. Clevers, Disease modeling in stem cell-derived 3D organoid systems. *Trends Mol. Med.* **23**, 393–410 (2017).
29. X. Yin, B. E. Mead, H. Safaee, R. Langer, J. M. Karp, O. Levy, Engineering stem cell organoids. *Cell Stem Cell* **18**, 25–38 (2016).
30. T. T. Pham, F. Giesert, A. Röthig, T. Floss, M. Kallnik, K. Weindl, S. M. Hölter, U. Ahting, H. Prokisch, L. Becker, T. Klopstock, M. H. de Angelis, K. Beyer, K. Görner, P. J. Kahle, D. M. Vogt Weisenhorn, W. Wurst, DJ-1-deficient mice show less TH-positive neurons in the ventral tegmental area and exhibit non-motoric behavioural impairments. *Genes Brain Behav.* **9**, 305–317 (2010).
31. J. S. Chandran, X. Lin, A. Zapata, A. Höke, M. Shimoji, S. O'Leary Moore, M. P. Galloway, F. M. Laird, P. C. Wong, D. L. Price, K. R. Bailey, J. N. Crawley, T. Shippenberg, H. Cai, Progressive behavioral deficits in *DJ-1*-deficient mice are associated with normal nigrostriatal function. *Neurobiol. Dis.* **29**, 505–514 (2008).
32. L. F. Burbulla, P. Song, J. R. Mazzulli, E. Zampese, Y. C. Wong, S. Jeon, D. P. Santos, J. Blanz, C. D. Obermaier, C. Strojny, J. N. Savas, E. Kiskinis, X. Zhuang, R. Krüger, D. J. Surmeier, D. Krainc, Dopamine oxidation mediates mitochondrial and lysosomal dysfunction in Parkinson's disease. *Science* **357**, 1255–1261 (2017).
33. R. B. Postuma, D. Berg, Advances in markers of prodromal Parkinson disease. *Nat. Rev. Neurol.* **12**, 622–634 (2016).
34. B. Lee, W. Rhead, G. A. Diaz, B. F. Scharschmidt, A. Mian, O. Shchelochkov, J. F. Marier, M. Beliveau, J. Mauney, K. Dickinson, A. Martinez, S. Gargosky, M. Mokhtarani, S. A. Berry, Phase 2 comparison of a novel ammonia scavenging agent with sodium phenylbutyrate in patients with urea cycle disorders: Safety, pharmacokinetics and ammonia control. *Mol. Genet. Metab.* **100**, 221–228 (2010).
35. T. Taira, K. Takahashi, R. Kitagawa, S. M. Iguchi-Ariga, H. Ariga, Molecular cloning of human and mouse DJ-1 genes and identification of Sp1-dependent activation of the human DJ-1 promoter. *Gene* **263**, 285–292 (2001).
36. M. Inden, Y. Kitamura, H. Takeuchi, T. Yanagida, K. Takata, Y. Kobayashi, T. Taniguchi, K. Yoshimoto, M. Kaneko, Y. Okuma, T. Taira, H. Ariga, S. Shimohama, Neurodegeneration of mouse nigrostriatal dopaminergic system induced by repeated oral administration of rotenone is prevented by 4-phenylbutyrate, a chemical chaperone. *J. Neurochem.* **101**, 1491–1504 (2007).
37. K. Ono, M. Ikemoto, T. Kawarabayashi, M. Ikeda, T. Nishinakagawa, M. Hosokawa, M. Shoji, M. Takahashi, M. Nakashima, A chemical chaperone, sodium 4-phenylbutyric acid, attenuates the pathogenic potency in human α-synuclein A30P+A53T transgenic mice. *Park. Relat. Disord.* **15**, 649–654 (2009).
38. R. Taipa, C. Pereira, I. Reis, I. Alonso, A. Bastos-Lima, M. Melo-Pires, M. Magalhães, DJ-1 linked parkinsonism (PARK7) is associated with Lewy body pathology. *Brain* **139**, 1680–1687 (2016).
39. F. B. Axelrod, L. Liebes, G. Gold-von Simson, S. Mendoza, J. Mull, M. Leyne, L. Norcliffe-Kaufmann, H. Kaufmann, S. A. Slaugenhaupt, Kinetin improves *IKBKAP* mRNA splicing in patients with familial dysautonomia. *Pediatr. Res.* **70**, 480–483 (2011).
40. R. S. Shetty, C. S. Gallagher, Y.-T. Chen, M. M. Hims, J. Mull, M. Leyne, J. Pickel, D. Kwok, S. A. Slaugenhaupt, Specific correction of a splice defect in brain by nutritional supplementation. *Hum. Mol. Genet.* **20**, 4093–4101 (2011).
41. V. La Cognata, V. D'Agata, F. Cavalcanti, S. Cavallaro, Splicing: Is there an alternative contribution to Parkinson's disease? *Neurogenetics* **16**, 245–263 (2015).
42. N. J. Schork, Personalized medicine: Time for one-person trials. *Nature* **520**, 609–611 (2015).
43. G. Yeo, C. B. Burge, Maximum entropy modeling of short sequence motifs with applications to RNA splicing signals. *J. Comput. Biol.* **11**, 377–394 (2004).
44. X. Jian, E. Boerwinkle, X. Liu, In silico prediction of splice-altering single nucleotide variants in the human genome. *Nucleic Acids Res.* **42**, 13534–13544 (2014).
45. X. Liu, C. Wu, C. Li, E. Boerwinkle, dbNSFP v3.0: A one-stop database of functional predictions and annotations for human nonsynonymous and splice-site SNVs. *Hum. Mutat.* **37**, 235–241 (2016).
46. J. R. Mazzulli, F. Zunke, O. Isacson, L. Studer, D. Krainc, α-Synuclein-induced lysosomal dysfunction occurs through disruptions in protein trafficking in human midbrain synucleinopathy models. *Proc. Natl. Acad. Sci. U.S.A.* **113**, 1931–1936 (2016).
47. K. Takahashi, K. Tanabe, M. Ohnuki, M. Narita, T. Ichisaka, K. Tomoda, S. Yamanaka, Induction of pluripotent stem cells from adult human fibroblasts by defined factors. *Cell* **131**, 861–872 (2007).
48. P. Reinhardt, B. Schmid, L. F. Burbulla, D. C. Schöndorf, L. Wagner, M. Glatza, S. Höing, G. Hargus, S. A. Heck, A. Dhingra, G. Wu, S. Müller, K. Brockmann, T. Kluba, M. Maisel, R. Krüger, D. Berg, Y. Tsytsyura, C. S. Thiel, O. E. Psathaki, J. Klingauf, T. Kuhlmann, M. Klewin, H. Müller, T. Gasser, H. R. Schöler, J. Sterneckert, Genetic correction of a LRRK2 mutation in human iPSCs links parkinsonian neurodegeneration to ERK-dependent changes in gene expression. *Cell Stem Cell* **12**, 354–367 (2013).
49. N. Weisschuh, B. Wissinger, E. Gramer, A splice site mutation in the PAX6 gene which induces exon skipping causes autosomal dominant inherited aniridia. *Mol. Vis.* **18**, 751–757 (2012).
50. S. Plum, S. Helling, C. Theiss, R. E. P. Leite, C. May, W. Jacob-Filho, M. Eisenacher, K. Kuhlmann, H. E. Meyer, P. Riederer, L. T. Grinberg, M. Gerlach, K. Marcus, Combined

enrichment of neuromelanin granules and synaptosomes from human substantia nigra pars compacta tissue for proteomic analysis. *J. Proteomics* **94**, 202–206 (2013).
51. M. Jinek, A. East, A. Cheng, S. Lin, E. Ma, J. Doudna, RNA-programmed genome editing in human cells. *eLife* **2**, e00471 (2013).
52. L. Cong, F. A. Ran, D. Cox, S. Lin, R. Barretto, N. Habib, P. D. Hsu, X. Wu, W. Jiang, L. A. Marraffini, F. Zhang, Multiplex genome engineering using CRISPR/Cas systems. *Science* **339**, 819–823 (2013).
53. M. A. DePristo, E. Banks, R. Poplin, K. V. Garimella, J. R. Maguire, C. Hartl, A. A. Philippakis, G. del Angel, M. A. Rivas, M. Hanna, A. McKenna, T. J. Fennell, A. M. Kernytsky, A. Y. Sivachenko, K. Cibulskis, S. B. Gabriel, D. Altshuler, M. J. Daly, A framework for variation discovery and genotyping using next-generation DNA sequencing data. *Nat. Genet.* **43**, 491–498 (2011).
54. The International HapMap Consortium, The International HapMap Project. *Nature* **426**, 789–796 (2003).
55. C. C. Chang, C. C. Chow, L. C. Tellier, S. Vattikuti, S. M. Purcell, J. J. Lee, Second-generation PLINK: Rising to the challenge of larger and richer datasets. *Gigascience* **4**, 7 (2015).
56. S. M. Purcell, J. L. Moran, M. Fromer, D. Ruderfer, N. Solovieff, P. Roussos, C. O'Dushlaine, K. Chambert, S. E. Bergen, A. Kähler, L. Duncan, E. Stahl, G. Genovese, E. Fernández, M. O. Collins, N. H. Komiyama, J. S. Choudhary, P. K. E. Magnusson, E. Banks, K. Shakir, K. Garimella, T. Fennell, M. DePristo, S. G. N. Grant, S. J. Haggarty, S. Gabriel, E. M. Scolnick, E. S. Lander, C. M. Hultman, P. F. Sullivan, S. A. McCarroll, P. Sklar, A polygenic burden of rare disruptive mutations in schizophrenia. *Nature* **506**, 185–190 (2014).
57. A. Manichaikul, J. C. Mychaleckyj, S. S. Rich, K. Daly, M. Sale, W.-M. Chen, Robust relationship inference in genome-wide association studies. *Bioinformatics* **26**, 2867–2873 (2010).
58. A. Tan, G. R. Abecasis, H. M. Kang, Unified representation of genetic variants. *Bioinformatics* **31**, 2202–2204 (2015).
59. H. Li, B. Handsaker, A. Wysoker, T. Fennell, J. Ruan, N. Homer, G. Marth, G. Abecasis, R. Durbin; 1000 Genome Project Data Processing Subgroup, The sequence alignment/map format and SAMtools. *Bioinformatics* **25**, 2078–2079 (2009).
60. Epi4K consortium; Epilepsy Phenome/Genome Project, Ultra-rare genetic variation in common epilepsies: A case-control sequencing study. *Lancet Neurol.* **16**, 135–143 (2017).
61. K. Wang, M. Li, H. Hakonarson, ANNOVAR: Functional annotation of genetic variants from high-throughput sequencing data. *Nucleic Acids Res.* **38**, –e164 (2010).
62. E. Marouli, M. Graff, C. Medina-Gomez, K. S. Lo, A. R. Wood, T. R. Kjaer, R. S. Fine, Y. Lu, C. Schurmann, H. M. Highland, S. Rüeger, G. Thorleifsson, A. E. Justice, D. Lamparter, K. E. Stirrups, V. Turcot, K. L. Young, T. W. Winkler, T. Esko, T. Karaderi, A. E. Locke, N. G. D. Masca, M. C. Y. Ng, P. Mudgal, M. A. Rivas, S. Vedantam, A. Mahajan, X. Guo, G. Abecasis, K. K. Aben, L. S. Adair, D. S. Alam, E. Albrecht, K. H. Allin, M. Allison, P. Amouyel, E. V. Appel, D. Arveiler, F. W. Asselbergs, P. L. Auer, B. Balkau, B. Banas, L. E. Bang, M. Benn, S. Bergmann, L. F. Bielak, M. Blüher, H. Boeing, E. Boerwinkle, C. A. Böger, L. L. Bonnycastle, J. Bork-Jensen, M. L. Bots, E. P. Bottinger, D. W. Bowden, I. Brandslund, G. Breen, M. H. Brilliant, L. Broer, A. A. Burt, A. S. Butterworth, D. J. Carey, M. J. Caulfield, J. C. Chambers, D. I. Chasman, Y.-D. I. Chen, R. Chowdhury, C. Christensen, A. Y. Chu, M. Cocca, F. S. Collins, J. P. Cook, J. Corley, J. C. Galbany, A. J. Cox, G. Cuellar-Partida, J. Danesh, G. Davies, P. I. W. de Bakker, G. J. de Borst, S. de Denus, M. C. H. de Groot, R. de Mutsert, I. J. Deary, G. Dedoussis, E. W. Demerath, A. I. den Hollander, J. G. Dennis, E. D. Angelantonio, F. Drenos, M. Du, A. M. Dunning, D. F. Easton, T. Ebeling, T. L. Edwards, P. T. Ellinor, P. Elliott, E. Evangelou, A.-E. Farmaki, J. D. Faul, M. F. Feitosa, S. Feng, E. Ferrannini, M. M. Ferrario, J. Ferrieres, J. C. Florez, I. Ford, M. Fornage, P. W. Franks, R. Frikke-Schmidt, T. E. Galesloot, W. Gan, I. Gandin, P. Gasparini, V. Giedraitis, A. Giri, G. Girotto, S. D. Gordon, P. Gordon-Larsen, M. Gorski, N. Grarup, M. L. Grove, V. Gudnason, S. Gustafsson, T. Hansen, K. M. Harris, T. B. Harris, A. T. Hattersley, C. Hayward, L. He, I. M. Heid, K. Heikkilä, Ø. Helgeland, J. Hernesniemi, A. W. Hewitt, L. J. Hocking, M. Hollensted, O. L. Holmen, G. Kees Hovingh, J. M. M. Howson, C. B. Hoyng, P. L. Huang, K. Hveem, M. Arfan Ikram, E. Ingelsson, A. U. Jackson, J.-H. Jansson, G. P. Jarvik, G. B. Jensen, M. A. Jhun, Y. Jia, X. Jiang, S. Johansson, M. E. Jørgensen, T. Jørgensen, P. Jousilahti, J. Wouter Jukema, B. Kahali, R. S. Kahn, M. Kähönen, P. R. Kamstrup, S. Kanoni, J. Kaprio, M. Karaleftheri, S. L. R. Kardia, F. Karpe, F. Kee, R. Keeman, L. A. Kiemeney, H. Kitajima, K. B. Kluivers, T. Kocher, P. Komulainen, J. Kontto, J. S. Kooner, C. Kooperberg, P. Kovacs, J. Kriebel, H. Kuivaniemi, S. Küry, J. Kuusisto, M. L. Bianca, M. Laakso, T. A. Lakka, E. M. Lange, L. A. Lange, C. D. Langefeld, C. Langenberg, E. B. Larson, I.-T. Lee, T. Lehtimäki, C. E. Lewis, H. Li, J. Li, R. Li-Gao, H. Lin, L.-A. Lin, X. Lin, L. Lind, J. Lindström, A. Linneberg, Y. Liu, Y. Liu, A. Lophatananon, J. Luan, S. A. Lubitz, L.-P. Lyytikäinen, D. A. Mackey, P. A. F. Madden, A. K. Manning, S. Männistö, G. Marenne, J. Marten, N. G. Martin, A. L. Mazul, K. Meidtner, A. Metspalu, P. Mitchell, K. L. Mohlke, D. O. Mook-Kanamori, A. Morgan, A. D. Morris, A. P. Morris, M. Müller-Nurasyid, P. B. Munroe, M. A. Nalls, M. Nauck, C. P. Nelson, M. Neville, S. F. Nielsen, K. Nikus, P. R. Njølstad, B. G. Nordestgaard, I. Ntalla, J. R. O'Connel, H. Oksa, L. M. Olde Loohuis, R. A. Ophoff, K. R. Owen, C. J. Packard, S. Padmanabhan, C. N. A. Palmer, G. Pasterkamp, A. P. Patel, A. Pattie, O. Pedersen, P. L. Peissig, G. M. Peloso, C. E. Pennell, M. Perola, J. A. Perry, J. R. B. Perry, T. N. Person, A. Pirie, O. Polasek, D. Posthuma, O. T. Raitakari, A. Rasheed, R. Rauramaa, D. F. Reilly, A. P. Reiner, F. Renström, P. M. Ridker, J. D. Rioux, N. Robertson, A. Robino, O. Rolandsson, I. Rudan, K. S. Ruth, D. Saleheen, V. Salomaa, N. J. Samani, K. Sandow, Y. Sapkota, N. Sattar, M. K. Schmidt, P. J. Schreiner, M. B. Schulze, R. A. Scott, M. P. Segura-Lepe, S. Shah, X. Sim, S. Sivapalaratnam, K. S. Small, A. V. Smith, J. A. Smith, L. Southam, T. D. Spector, E. K. Speliotes, J. M. Starr, V. Steinthorsdottir, H. M. Stringham, M. Stumvoll, P. Surendran, L. M. 't Hart, K. E. Tansey, J.-C. Tardif, K. D. Taylor, A. Teumer, D. J. Thompson, U. Thorsteinsdottir, B. H. Thuesen, A. Tönjes, G. Tromp, S. Trompet, E. Tsafantakis, J. Tuomilehto, A. Tybjaerg-Hansen, J. P. Tyrer, R. Uher, A. G. Uitterlinden, S. Ulivi, S. W. van der Laan, A. R. Van Der Leij, C. M. van Duijn, N. M. van Schoor, J. van Setten, A. Varbo, T. V. Varga, R. Varma, D. R. Velez Edwards, S. H. Vermeulen, H. Vestergaard, V. Vitart, T. F. Vogt, D. Vozzi, M. Walker, F. Wang, C. A. Wang, S. Wang, Y. Wang, N. J. Wareham, H. R. Warren, J. Wessel, S. M. Willems, J. G. Wilson, D. R. Witte, M. O. Woods, Y. Wu, H. Yaghootkar, J. Yao, P. Yao, L. M. Yerges-Armstrong, R. Young, E. Zeggini, X. Zhan, W. Zhang, J. H. Zhao, W. Zhao, W. Zhao, H. Zheng, W. Zhou; The EPIC-Inter Act Consortium; CHD Exome+ Consortium; Exome BP Consortium; TD-Genes Consortium; Go TD Genes Consortium; Global Lipids Genetics Consortium; ReproGen Consortium; MAGIC Investigators, J. I. Rotter, M. Boehnke, S. Kathiresan, M. I. Mc Carthy, C. J. Willer, K. Stefansson, I. B. Borecki, D. J. Liu, K. E. North, N. L. Heard-Costa, T. H. Pers, C. M. Lindgren, C. Oxvig, Z. Kutalik, F. Rivadeneira, R. J. F. Loos, T. M. Frayling, J. N. Hirschhorn, P. Deloukas, G. Lettre, Rare and low-frequency coding variants alter human adult height. *Nature* **542**, 186–190 (2017).
63. 1000 Genomes Project Consortium, A global reference for human genetic variation. *Nature* **526**, 68–74 (2015).
64. M. Lek, K. J. Karczewski, E. V. Minikel, K. E. Samocha, E. Banks, T. Fennell, A. H. O'Donnell-Luria, J. S. Ware, A. J. Hill, B. B. Cummings, T. Tukiainen, D. P. Birnbaum, J. A. Kosmicki, L. E. Duncan, K. Estrada, F. Zhao, J. Zou, E. Pierce-Hoffman, J. Berghout, D. N. Cooper, N. Deflaux, M. De Pristo, R. Do, J. Flannick, M. Fromer, L. Gauthier, J. Goldstein, N. Gupta, D. Howrigan, A. Kiezun, M. I. Kurki, A. L. Moonshine, P. Natarajan, L. Orozco, G. M. Peloso, R. Poplin, M. A. Rivas, V. Ruano-Rubio, S. A. Rose, D. M. Ruderfer, K. Shakir, P. D. Stenson, C. Stevens, B. P. Thomas, G. Tiao, M. T. Tusie-Luna, B. Weisburd, H.-H. Won, D. Yu, D. M. Altshuler, D. Ardissino, M. Boehnke, J. Danesh, S. Donnelly, R. Elosua, J. C. Florez, S. B. Gabriel, G. Getz, S. J. Glatt, C. M. Hultman, S. Kathiresan, M. Laakso, S. M. Carroll, M. I. McCarthy, D. M. Govern, R. M. Pherson, B. M. Neale, A. Palotie, S. M. Purcell, D. Saleheen, J. M. Scharf, P. Sklar, P. F. Sullivan, J. Tuomilehto, M. T. Tsuang, H. C. Watkins, J. G. Wilson, M. J. Daly, D. G. MacArthur; Exome Aggregation Consortium, Analysis of protein-coding genetic variation in 60,706 humans. *Nature* **536**, 285–291 (2016).
65. M. D. Shirley, Z. Ma, B. S. Pedersen, S. J. Wheelan, Efficient "pythonic" access to FASTA files using pyfaidx. *PeerJ PrePrints* **3**, e1196 (2015).
66. B. M. Rossi, E. I. Palmero, F. López-Kostner, C. Sarroca, C. A. Vaccaro, F. Spirandelli, P. Ashton-Prolla, Y. Rodriguez, H. de Campos Reis Galvão, R. M. Reis, A. Escremim de Paula, L. G. Capochin Romagnolo, K. Alvarez, A. Della Valle, F. Neffa, P. G. Kalfayan, E. Spirandelli, S. Chialina, M. Gutiérrez Angulo, M. D. C. Castro-Mujica, J. Sanchez de Monte, R. Quispe, S. D. da Silva, N. T. Rossi, C. Barletta-Carrillo, S. Revollo, X. Taborga, L. L. Morillas, H. Tubeuf, E. M. Monteiro-Santos, T. A. Piñero, C. Dominguez-Barrera, P. Wernhoff, A. Martins, E. Hovig, P. Møller, M. Dominguez-Valentin, A survey of the clinicopathological and molecular characteristics of patients with suspected Lynch syndrome in Latin America. *BMC Cancer* **17**, 623 (2017).
67. B. Wappenschmidt, A. A. Becker, J. Hauke, U. Weber, S. Engert, J. Köhler, K. Kast, N. Arnold, K. Rhiem, E. Hahnen, A. Meindl, R. K. Schmutzler, Analysis of 30 putative BRCA1 splicing mutations in hereditary breast and ovarian cancer families identifies exonic splice site mutations that escape in silico prediction. *PLOS ONE* **7**, e50800 (2012).
68. P. D. Stenson, E. V. Ball, M. Mort, A. D. Phillips, J. A. Shiel, N. S. T. Thomas, S. Abeysinghe, M. Krawczak, D. N. Cooper, Human Gene Mutation Database (HGMD®): 2003 update. *Hum. Mutat.* **21**, 577–581 (2003).
69. D. Pinto, E. Delaby, D. Merico, M. Barbosa, A. Merikangas, L. Klei, B. Thiruvahindrapuram, X. Xu, R. Ziman, Z. Wang, J. A. S. Vorstman, A. Thompson, R. Regan, M. Pilorge, G. Pellecchia, A. T. Pagnamenta, B. Oliveira, C. R. Marshall, T. R. Magalhaes, J. K. Lowe, J. L. Howe, A. J. Griswold, J. Gilbert, E. Duketis, B. A. Dombroski, M. V. De Jonge, M. Cuccaro, E. L. Crawford, C. T. Correia, J. Conroy, I. C. Conceição, A. G. Chiocchetti, J. P. Casey, G. Cai, C. Cabrol, N. Bolshakova, E. Bacchelli, R. Anney, S. Gallinger, M. Cotterchio, G. Casey, L. Zwaigenbaum, K. Wittemeyer, K. Wing, S. Wallace, H. van Engeland, A. Tryfon, S. Thomson, L. Soorya, B. Rogé, W. Roberts, F. Poustka, S. Mouga, N. Minshew, L. A. McInnes, S. G. McGrew, C. Lord, M. Leboyer, A. S. Le Couteur, A. Kolevzon, P. J. González, S. Jacob, R. Holt, S. Guter, J. Green, A. Green, C. Gillberg, B. A. Fernandez, F. Duque, R. Delorme, G. Dawson, P. Chaste, C. Café, S. Brennan, T. Bourgeron, P. F. Bolton, S. Bölte, R. Bernier, G. Baird, A. J. Bailey, E. Anagnostou, J. Almeida, E. M. Wijsman, V. J. Vieland, A. M. Vicente, G. D. Schellenberg, M. Pericak-Vance, A. D. Paterson, J. R. Parr, G. Oliveira, J. I. Nurnberger, A. P. Monaco, E. Maestrini, S. M. Klauck, H. Hakonarson, J. L. Haines, D. H. Geschwind, C. M. Freitag, S. E. Folstein, S. Ennis, H. Coon, A. Battaglia, P. Szatmari, J. S. Sutcliffe, J. Hallmayer, M. Gill,

E. H. Cook, J. D. Buxbaum, B. Devlin, L. Gallagher, C. Betancur, S. W. Scherer, Convergence of genes and cellular pathways dysregulated in autism spectrum disorders. *Am. J. Hum. Genet.* **94**, 677–694 (2014).

70. G. Genovese, M. Fromer, E. A. Stahl, D. M. Ruderfer, K. Chambert, M. Landén, J. L. Moran, S. M. Purcell, P. Sklar, P. F. Sullivan, C. M. Hultman, S. A. McCarroll, Increased burden of ultra-rare protein-altering variants among 4,877 individuals with schizophrenia. *Nat. Neurosci.* **19**, 1433–1441 (2016).
71. S. Dong, M. F. Walker, N. J. Carriero, M. DiCola, A. J. Willsey, A. Y. Ye, Z. Waqar, L. E. Gonzalez, J. D. Overton, S. Frahm, J. F. Keaney III, N. A. Teran, J. Dea, J. D. Mandell, V. Hus Bal, C. A. Sullivan, N. M. DiLullo, R. O. Khalil, J. Gockley, Z. Yuksel, S. M. Sertel, A. G. Ercan-Sencicek, A. R. Gupta, S. M. Mane, M. Sheldon, A. I. Brooks, K. Roeder, B. Devlin, M. W. State, L. Wei, S. J. Sanders, De novo insertions and deletions of predominantly paternal origin are associated with autism spectrum disorder. *Cell Rep.* **9**, 16–23 (2014).
72. A. Ganna, G. Genovese, D. P. Howrigan, A. Byrnes, M. I. Kurki, S. M. Zekavat, C. W. Whelan, M. Kals, M. G. Nivard, A. Bloemendal, J. M. Bloom, J. I. Goldstein, T. Poterba, C. Seed, R. E. Handsaker, P. Natarajan, R. Mägi, D. Gage, E. B. Robinson, A. Metspalu, V. Salomaa, J. Suvisaari, S. M. Purcell, P. Sklar, S. Kathiresan, M. J. Daly, S. A. McCarroll, P. F. Sullivan, A. Palotie, T. Esko, C. M. Hultman, B. M. Neale, Ultra-rare disruptive and damaging mutations influence educational attainment in the general population. *Nat. Neurosci.* **19**, 1563–1565 (2016).
73. S. J. Sanders, X. He, A. J. Willsey, A. G. Ercan-Sencicek, K. E. Samocha, A. E. Cicek, M. T. Murtha, V. H. Bal, S. L. Bishop, S. Dong, A. P. Goldberg, C. Jinlu, J. F. Keaney III, L. Klei, J. D. Mandell, D. Moreno-de-Luca, C. S. Poultney, E. B. Robinson, L. Smith, T. Solli-Nowlan, M. Y. Su, N. A. Teran, M. F. Walker, D. M. Werling, A. L. Beaudet, R. M. Cantor, E. Fombonne, D. H. Geschwind, D. E. Grice, C. Lord, J. K. Lowe, S. M. Mane, D. M. Martin, E. M. Morrow, M. E. Talkowski, J. S. Sutcliffe, C. A. Walsh, T. W. Yu; Autism Sequencing Consortium, D. H. Ledbetter, C. L. Martin, E. H. Cook, J. D. Buxbaum, M. J. Daly, B. Devlin, K. Roeder, M. W. State, Insights into autism spectrum disorder genomic architecture and biology from 71 risk loci. *Neuron* **87**, 1215–1233 (2015).
74. S. T. Sherry, M. H. Ward, M. Kholodov, J. Baker, L. Phan, E. M. Smigielski, K. Sirotkin, dbSNP: The NCBI database of genetic variation. *Nucleic Acids Res.* **29**, 308–311 (2001).
75. T. Singh, M. I. Kurki, D. Curtis, S. M. Purcell, L. Crooks, J. M. Rae, J. Suvisaari, H. Chheda, D. Blackwood, G. Breen, O. Pietiläinen, S. S. Gerety, M. Ayub, M. Blyth, T. Cole, D. Collier, E. L. Coomber, N. Craddock, M. J. Daly, J. Danesh, M. D. Forti, A. Foster, N. B. Freimer, D. Geschwind, M. Johnstone, S. Joss, G. Kirov, J. Körkkö, O. Kuismin, P. Holmans, C. M. Hultman, C. Iyegbe, J. Lönnqvist, M. Männikkö, S. A. McCarroll, P. M. Guffin, A. M. McIntosh, A. M. Quillin, J. S. Moilanen, C. Moore, R. M. Murray, R. Newbury-Ecob, W. Ouwehand, T. Paunio, E. Prigmore, E. Rees, D. Roberts, J. Sambrook, P. Sklar, D. S. Clair, J. Veijola, J. T. R. Walters, H. Williams; Swedish Schizophrenia Study; INTERVAL Study; DDD Study; UK10 K Consortium, P. F. Sullivan, M. E. Hurles, M. C. O'Donovan, A. Palotie, M. J. Owen, J. C. Barrett, Rare loss-of-function variants in *SETD1A* are associated with schizophrenia and developmental disorders. *Nat. Neurosci.* **19**, 571–577 (2016).
76. S. I. O'Donoghue, H. Horn, E. Pafilis, S. Haag, M. Kuhn, V. P. Satagopam, R. Schneider, L. J. Jensen, Reflect: A practical approach to web semantics. *Web Semant.* **8**, 182–189 (2010).
77. J.-D. Kim, T. Ohta, Y. Tateisi, J. Tsujii, GENIA corpus—A semantically annotated corpus for bio-textmining. *Bioinformatics* **19**, i180–i182 (2003).
78. Y. Tsuruoka, Y. Tateishi, J.-D. Kim, T. Ohta, J. M. Naught, S. Ananiadou, J. Tsujii, Developing a robust part-of-speech tagger for biomedical text. *Advances in Informatics* **2005**, 382–392 (2005).
79. D. Klein, C. D. Manning, in *Proceedings of the 41st Annual Meeting on Association for Computational Linguistics - ACL '03* (Association for Computational Linguistics, 2003), vol. 1, pp. 423–430.

Acknowledgments: Genetic analyses presented in this paper were carried out using the HPC facilities of the University of Luxembourg (http://hpc.uni.lu). We would like to thank the Michael J. Fox Foundation and the PDGSC (Parkinson Disease Genetic Sequencing Consortium) for providing access to their datasets (for a full list of members and funding sources of the PDGSC, please see the Supplementary Materials). **Funding:** This work was supported by grants from the Luxembourg National Research Fund (FNR) within the PEARL programme (FNR; FNR/P13/6682797 to R.K.), the German Research Council (DFG; KR2119/8-1 to R.K. and T.G. and KL1134/11-1 to C.K.), the EU Joint Program-Neurodegenerative Diseases (JPND; COURAGE-PD to E.G., D.R.B., P.M., R.K., C.K., and T.G.; 3DPD to J.C.S.), and the European Union's Horizon2020 research and innovation program under grant agreement no. 692320 (WIDESPREAD; CENTRE-PD to R.K.). This work was supported by NIH grants R01NS076054 and R37 NS096241 (to D.K.). The work was supported by the Luxembourg National Research Fund (FNR; grant no. C13/BM/5782168) to E.G. Works of C.M. and K.M. were supported by the HUPO Brain Proteome Project, PURE (a project of Nordrhein-Westfalen, a federal German state), the Deutsche Parkinson Gesellschaft e.V., and the Verein zur Durchführung Neurowissenschaftlicher Tagungen e.V. (Berlin, Germany). Work was supported by the German Science Foundation Collaborative Research Centre (CRC 870to W.W.) on "DJ-1 Linked Neurodegeneration Pathways in New Mouse Models of Parkinson's Disease" (WU 164/5-1 to W.W.); Munich Cluster for Systems Neurology (EXC 1010 SyNergy to W.W.); the Bavarian Ministry of Education, Culture and Science [Human Induced Pluripotent Stem Cells (ForIPS)]; the Helmholtz Portfolio Theme "Supercomputing and Modelling for the Human Brain" (SMHB); and the German Federal Ministry of Education and Research (BMBF) within the framework of the e:Med research and funding concept MitoPD (grant 031A430E to W.W.). C.K. is the recipient of a career development award from the Hermann and Lilly Schilling Foundation. **Author contributions:** I.B., C.D.O., and R.K. designed the overall study. I.B., C.D.O., Z.H., A.L., F.M., G.C., S.D., and R.K. designed and/or performed all experiments including iPSC, smNPC, in vitro expression of DJ-1, and all drug screenings. I.B., C.D.O., D.G., L.F.B., J.B., B.S., T.G., D.K., and R.K. designed and/or performed the experiments including establishing patient-derived fibroblast lines and phenotyping of those fibroblasts. S.B. and J.C.S. designed and performed the organoid experiments. N.W., F.G., A.K.-D., D.M.V.W., and W.W. designed and performed the gene editing of the patient-derived fibroblasts. L.D.C. and M. Baralle designed and performed the Northern blot and fractionation experiments. C.M. and K.M. designed and performed the mass spectrometry. K.W. and B.W. performed and analyzed the retargeted sequencing of the PARK7 locus of the index patient. C.K. provided the control cells used in this study. E.G. modeled RNA structure. M. Biryukov performed the computational literature mining. D.R.B. and P.M. performed the burden analysis. D.W. and R.K. performed the clinical examination of DJ-1 mutation carriers and provided biomaterial. I.B. and R.K. wrote the manuscript, with the assistance of all coauthors. **Competing interests:** The University of Luxembourg has filed a patent: Luxembourg patent no. 93116 "MEANS AND METHODS FOR TREATING PARKINSON'S DISEASE." R.K., I.B., and C.D.O. are listed as inventors. J.C.S. is cofounder (including shares) and CEO of OrganoTherapeutics SARL. D.K. is the founder and Scientific Advisory Board Chair of Lysosomal Therapeutics Inc. He serves on the scientific advisory boards of The Silverstein Foundation, Intellia Therapeutics, and Prevail Therapeutics and is a Venture Partner at OrbiMed. M. A. Nalls' participation is supported by a consulting contract between Data Tecnica International LLC and the National Institute on Aging, NIH, Bethesda, MD, USA. M. A. Nalls also consults for Genoom Health, Illumina Inc., The Michael J. Fox Foundation for Parkinson's Research, and University of California Health Care, among others. **Data and materials availability:** All data associated with this study are present in the paper or the Supplementary Materials.

Submitted 6 June 2018
Resubmitted 24 January 2020
Accepted 22 June 2020
Published 9 September 2020
10.1126/scitranslmed.aau3960

Citation: I. Boussaad, C. D. Obermaier, Z. Hanss, D. R. Bobbili, S. Bolognin, E. Glaab, K. Wołyńska, N. Weisschuh, L. De Conti, C. May, F. Giesert, D. Grossmann, A. Lambert, S. Kirchen, M. Biryukov, L. F. Burbulla, F. Massart, J. Bohler, G. Cruciani, B. Schmid, A. Kurz-Drexler, P. May, S. Duga, C. Klein, J. C. Schwamborn, K. Marcus, D. Woitalla, D. M. Vogt Weisenhorn, W. Wurst, M. Baralle, D. Krainc, T. Gasser, B. Wissinger, R. Krüger, A patient-based model of RNA mis-splicing uncovers treatment targets in Parkinson's disease. *Sci. Transl. Med.* **12**, eaau3960 (2020).

Science Translational Medicine

A patient-based model of RNA mis-splicing uncovers treatment targets in Parkinson's disease

Ibrahim Boussaad, Carolin D. Obermaier, Zoé Hanss, Dheeraj R. Bobbili, Silvia Bolognin, Enrico Glaab, Katarzyna Wolynska, Nicole Weisschuh, Laura De Conti, Caroline May, Florian Giesert, Dajana Grossmann, Annika Lambert, Susanne Kirchen, Maria Biryukov, Lena F. Burbulla, Francois Massart, Jill Bohler, Gérald Cruciani, Benjamin Schmid, Annerose Kurz-Drexler, Patrick May, Stefano Duga, Christine Klein, Jens C. Schwamborn, Katrin Marcus, Dirk Woitalla, Daniela M. Vogt Weisenhorn, Wolfgang Wurst, Marco Baralle, Dimitri Krainc, Thomas Gasser, Bernd Wissinger and Rejko Krüger

Sci Transl Med **12**, eaau3960.
DOI: 10.1126/scitranslmed.aau3960

PARK(7) preservation

Mutations in PARK7 lead to the development of early-onset Parkinson's disease (PD), a neurodegenerative condition for which there are currently no effective treatments. Here, Boussaad *et al.* identified an exonic splicing mutation in PARK7 linked to PD and studied the effect of this mutation in patient-derived cellular models. The mutation resulted in impaired splicing, reduced production of DJ-1 protein, and consequent mitochondrial dysfunction. Rescuing the aberrant splicing with the kinetin analog RECTAS in combination with phenylbutyric acid rescued neuronal loss in patient-derived brain organoids. The results suggest that precision medicine targeting specific molecular signatures could be an effective strategy for PD and possibly other neurodegenerative diseases.